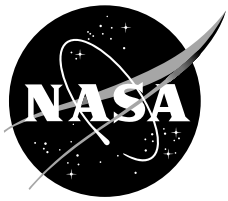


NASA/TM-1999-208789



Blade-Vortex Interaction Noise of a Full-Scale XV-15 Rotor Tested in the NASA Ames 80- by 120-Foot Wind Tunnel

C. Kitaplioglu

The NASA STI Program Office . . . in Profile

Since its founding, NASA has been dedicated to the advancement of aeronautics and space science. The NASA Scientific and Technical Information (STI) Program Office plays a key part in helping NASA maintain this important role.

The NASA STI Program Office is operated by Langley Research Center, the Lead Center for NASA's scientific and technical information. The NASA STI Program Office provides access to the NASA STI Database, the largest collection of aeronautical and space science STI in the world. The Program Office is also NASA's institutional mechanism for disseminating the results of its research and development activities. These results are published by NASA in the NASA STI Report Series, which includes the following report types:

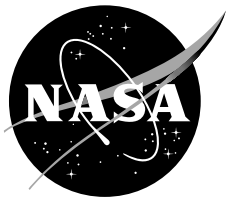
- **TECHNICAL PUBLICATION.** Reports of completed research or a major significant phase of research that present the results of NASA programs and include extensive data or theoretical analysis. Includes compilations of significant scientific and technical data and information deemed to be of continuing reference value. NASA's counterpart of peer-reviewed formal professional papers but has less stringent limitations on manuscript length and extent of graphic presentations.
- **TECHNICAL MEMORANDUM.** Scientific and technical findings that are preliminary or of specialized interest, e.g., quick release reports, working papers, and bibliographies that contain minimal annotation. Does not contain extensive analysis.
- **CONTRACTOR REPORT.** Scientific and technical findings by NASA-sponsored contractors and grantees.
- **CONFERENCE PUBLICATION.** Collected papers from scientific and technical conferences, symposia, seminars, or other meetings sponsored or cosponsored by NASA.
- **SPECIAL PUBLICATION.** Scientific, technical, or historical information from NASA programs, projects, and missions, often concerned with subjects having substantial public interest.
- **TECHNICAL TRANSLATION.** English-language translations of foreign scientific and technical material pertinent to NASA's mission.

Specialized services that complement the STI Program Office's diverse offerings include creating custom thesauri, building customized databases, organizing and publishing research results . . . even providing videos.

For more information about the NASA STI Program Office, see the following:

- Access the NASA STI Program Home Page at <http://www.sti.nasa.gov>
- E-mail your question via the Internet to help@sti.nasa.gov
- Fax your question to the NASA Access Help Desk at (301) 621-0134
- Telephone the NASA Access Help Desk at (301) 621-0390
- Write to:
NASA Access Help Desk
NASA Center for AeroSpace Information
7121 Standard Drive
Hanover, MD 21076-1320

NASA/TM-1999-208789



Blade-Vortex Interaction Noise of a Full-Scale XV-15 Rotor Tested in the NASA Ames 80- by 120-Foot Wind Tunnel

C. Kitaplioglu

Ames Research Center, Moffett Field, California

National Aeronautics and
Space Administration

Ames Research Center
Moffett Field, California 94035-1000

July 1999

NOTICE

Use of trade names or names of manufacturers in this document does not constitute an official endorsement of such products or manufacturers, either expressed or implied, by the National Aeronautics and Space Administration.

Available from:

NASA Center for AeroSpace Information
7121 Standard Drive
Hanover, MD 21076-1320
(301) 621-0390

National Technical Information Service
5285 Port Royal Road
Springfield, VA 22161
(703) 487-4650

BLADE-VORTEX INTERACTION NOISE OF A FULL-SCALE XV-15 ROTOR TESTED IN THE NASA AMES 80- BY 120-FOOT WIND TUNNEL

C. Kitaplioglu

Ames Research Center

SUMMARY

A full-scale isolated XV-15 rotor was tested in the NASA Ames 80- by 120-Foot Wind Tunnel to determine the baseline blade-vortex interaction (BVI) noise signature at typical descending flight conditions. The test is briefly described. Representative samples of the acoustic data are presented. All of the acoustic data are included on an enclosed CD-ROM.

NOMENCLATURE

BLSPL	Band-Limited Sound Pressure Level
CT	rotor thrust coefficient
CQ	rotor torque coefficient
dBA	A-weighted Sound Pressure Level
M _{tip}	rotor tip Mach number
OASPL	Overall Sound Pressure Level
p	sound pressure
R	rotor radius
V _∞	tunnel velocity
X _m	streamwise location of microphone traverse
α _s	rotor shaft angle, deg (α _s is measured from normal to tunnel flow)
α _{TPP}	rotor tip-path-plane angle, deg

β_{1C} blade longitudinal flapping angle, deg

μ rotor advance ratio

σ rotor solidity

TEST OBJECTIVES AND APPROACH

An isolated, full-scale XV-15 rotor was tested in the NASA Ames 80- by 120-Foot Wind Tunnel (fig. 1) of the National Full-Scale Aerodynamics Complex (NFAC) to establish the baseline blade-vortex interaction (BVI) noise signature of a full-scale tiltrotor in descending flight. This was accomplished by systematically varying the rotor advance ratio and tip path plane angle for several fixed values of rotor thrust coefficient and tip Mach number. Another major objective of the test was to validate these wind tunnel data against similar data obtained on the XV-15 aircraft in flight (ref. 1). For this purpose the rotor was operated in the wind tunnel in a manner to closely simulate the state of the rotor in flight under the same operating conditions.

Because of the highly directional nature of BVI noise (for counterclockwise rotation BVI noise has a peak directivity angle to starboard and down from the rotor plane) and the opposite rotation of the two rotors (and, therefore, their highly divergent peak BVI directivities) on an XV-15 aircraft, the BVI noise of one rotor has little contribution in the direction where the BVI noise of the opposite rotor is dominant. This allowed an effective comparison of an isolated rotor tested in the wind tunnel with a full aircraft tested in flight.

To measure the BVI noise field of the rotor, a microphone was placed at a position of estimated peak BVI noise directivity, identical during both the in-flight test and the wind tunnel test. A second microphone was used in the wind tunnel to test the validity of simulating the BVI noise field of a dual tilt rotor with a single rotor.

An additional set of microphones mounted on a traverse in the wind tunnel was used to characterize the acoustic footprint under the advancing side of the rotor.

An analysis of the acoustic data and comparison to flight test data were presented in reference 1. Analyses of the rotor performance data were presented in references 2 and 3. This technical memorandum presents the complete acoustic data set.

TEST DESCRIPTION

Test Hardware

A single, full-scale, XV-15 rotor was tested on the Ames Rotor Test Apparatus (RTA). The rotation direction of the rotor was the same as the starboard rotor of the aircraft. The RTA is a special-purpose

test stand for operating full-scale rotors in the NFAC. The RTA houses electric drive motors, a right-angle transmission, a five-component rotor balance, and primary and dynamic control systems. The RTA was mounted in the wind tunnel on a three-strut support system placing the rotor hub 31 ft (2.5 rotor radii) above the tunnel floor. The rotor shaft angle could be changed by adjusting the height of the tail strut. The rotor hub center was 11.58 ft above the pitch axis.

The XV-15 rotor has three highly twisted, metal blades with a radius of 12.5 ft. The rotor and blade characteristics are summarized in table 1. More detailed descriptions can be found in reference 4. Rotor collective and cyclic pitch controls were input through the swashplate by three electro-mechanical/hydraulic actuators.

The wind tunnel test section walls are treated with acoustically absorbent material to reduce reflections that can contaminate the noise field. This provides an absorptivity of greater than 90% down to a frequency of approximately 250 Hz. To reduce contamination by hard surfaces on the test model and hardware, additional absorptive material was added to the Rotor Test Apparatus, the struts, the microphone traverse, and selected hard spots on the test section floor.

Instrumentation and Data Acquisition

Figure 2 shows the arrangement of the microphones in the wind tunnel test section. Figure 3 illustrates the coordinate system. The origin is coincident with the rotor hub center when the shaft angle is set to zero ($\alpha_s = 0$). The positions of the microphones are given in table 2. Microphones #1 through #4 were mounted on a streamwise traversing mechanism to probe the acoustic footprint under the advancing side of the rotor where the highest BVI noise levels would be encountered. Microphone #5 was placed at a position of estimated peak BVI noise directivity. Microphone #6 was positioned to simulate the measurement of the noise of the second rotor at Microphone #5.

Instrumentation-grade 0.5-in. condenser microphones (Brüel & Kjaer type 4133) were used for the acoustic measurements. The microphone signals were preamplified at the source to minimize signal loss over the long wiring runs. Microphone power supplies provided proper impedance matching. The signals were further amplified to maximize signal-to-noise ratio at the measurement system. In addition to the microphone signals, encoders on the rotor shaft provided a 1/rev trigger signal, as well as a 2048/rev clocking signal.

The data acquisition system consisted of anti-aliasing filters and 16-bit digitizers. The data were digitized at 2048 samples/revolution (20480 samples/sec at a nominal RPM of 600) using the clocking signal from the rotor encoder. All channels were triggered and sampled simultaneously. The anti-aliasing filters were set at a cutoff frequency of 4 kHz for the rotor operating at 600 RPM.

Sixteen revolutions of data were digitized and stored at each test condition. Preliminary processing of the data after the completion of each run provided an averaged time history and power spectrum for each microphone. A dBA metric was also calculated and provided guidance for choice of a test matrix for subsequent data runs.

An end-to-end calibration of each microphone channel was performed prior to each data run. A fixed frequency pistonphone (Brüel & Kjaer type 4220) of known output (nominally 124 dB at 250 Hz) traceable to the NASA Ames Calibration Lab was utilized for the calibrations. These calibrations provided engineering units conversions that were updated prior to the run.

Test Matrix

The initial task was to map out the BVI noise variations as a function of rotor operating condition and to locate the operating condition at which maximum BVI noise occurred. This was done at fixed rotor tip Mach number and fixed thrust coefficient, while varying rotor tip-path-plane angle and advance ratio. Once this was accomplished, the next steps were to obtain the advancing side acoustic footprint at the peak BVI condition and to document how the acoustic field changed with operating parameters from this peak BVI noise condition.

The relatively quick preliminary processing of data allowed a strategy of successive refinement of the test matrix as the test progressed and data accumulated. During this phase of testing, the rotor was trimmed to zero flapping, so that the rotor tip-path-plane angle was essentially equal to the shaft angle.

Matching wind tunnel test conditions with those measured during flight required a different approach. The rotor trim state was not matched exactly between the wind tunnel and flight test. The longitudinal flapping on the aircraft results from balancing aircraft moments for a given flight condition. These values of longitudinal flapping were not obtained in the wind tunnel due to control system load constraints. Therefore, the rotor tip-path-plane angle ($\alpha_{TPP} = \alpha_S + \beta_1 C$) was matched between the two tests, rather than the shaft angle and longitudinal flapping individually. As there was no direct measure of rotor thrust on the aircraft, and estimating the rotor thrust from the aircraft weight and wing lift was problematic, the rotor torque coefficient was used as a matching parameter. The rotor torque is a direct measurement from the rotor shaft for both the XV-15 aircraft and the wind tunnel model. It was assumed that by matching μ , M_{tip} , α_{TPP} , and C_Q , the rotor thrust for the two tests would be equal.

Table 3 shows the complete test matrix. The table has been sorted by operating condition, rather than by test sequence. Surveys of the acoustic field under the advancing side of the rotor are outlined in dark. Lighter outlines delineate operating parameters of constant value.

TEST DATA

Data Processing

During data acquisition, 16 revolutions of data, each revolution consisting of 2048 points, were digitized and written to disk. Initial examination of the data showed excellent rev-to-rev repeatability of the data as illustrated in figure 4(a), which includes each individual revolution of data (light lines) as well as the averaged data (dark line). The high amplitude pulses indicative of the BVI events have identical azimuth phases when each revolution of the total 16 revolution record is superimposed as detailed on figures 4(b), 4(c), and 4(d). Therefore, a straightforward synchronous average of the data

in the time domain, based on the 1/rev trigger, preserves the pulse-like nature of the BVI events. The overall procedure for post-test processing of the data is illustrated in figure 5. The 16 revolutions of time history data were synchronously averaged based on the 1/rev trigger pulses, resulting in an averaged time history of one revolution duration of 2048 points. The Fourier transform of this averaged time history yielded a power spectrum of 1/rev resolution (10 Hz for 600 RPM). An additional step yielded an A-weighted Sound Power Spectrum. The averaged time history was filtered, as described in the next paragraph, to focus on the BVI event. Three noise level metrics were obtained by integrating the respective sound pressure power spectra: OASPL from the unfiltered spectra, dBA from the A-weighted power spectra, and BLSPS from the bandpass filtered spectra.

Figure 6 compares the time history of a high BVI noise case to one where BVI noise is essentially absent. The main feature of the BVI is the high amplitude double pulse. To highlight these BVI events, the averaged time history was digitally filtered to attenuate frequency content below the 10th and above the 50th blade passage harmonics. The 10th harmonic was selected for the lower cutoff frequency, rather than the 5th harmonic used by some investigators (e.g. ref. 5), because of the potential contamination of the lower frequency components by wind tunnel reflections as well as wind tunnel drive fan noise. The 50th harmonic (rather than the 40th) was selected to include significant BVI acoustic energy at the higher frequencies. Figure 7 compares data that were bandpass filtered to include the 10th to 50th blade passage harmonics to the same data filtered to include the 5th to 40th harmonics, and to unfiltered data. The figure illustrates that the selected method of bandpass filtering the 10th to 50th harmonics adequately preserves the peak-to-peak amplitude and pulse width of the high amplitude acoustic pulse indicative of the BVI event, while effectively attenuating the (potentially contaminated) low frequency content unrelated to BVI.

Data Quality

Several aspects of data quality are discussed. As mentioned in the “Test Hardware” section, in addition to the sound-absorbing material permanently installed in the wind tunnel test section walls, additional foam was added to minimize reflections from the test hardware. To test the efficacy of this additional treatment, an impulsive sound source (a starter pistol), located at estimated BVI source positions, was used to check for the presence of reflections before and after the application of the additional treatment.

Figure 8 illustrates a typical case at Microphone #5. Prior to treatment (Fig 8(a)), a strong reflected pulse is present at a delay time (from the direct pulse) of 4 msec. This represents a path length difference between the direct and reflected signals of approximately 4.5 ft at a source-to-receiver distance of 75 ft, indicating that the reflection point was most likely somewhere on the surface of the test model fuselage. There are several other, weaker, reflections, most likely from tunnel floor hard points. After covering with foam the portion of the fuselage on the side facing the microphones (the forward, advancing side), we show, in figure 8(b), that the primary reflection was effectively eliminated. We were less successful in eliminating the other, weaker reflections, presumably because we were unable to pinpoint the reflection points. Although some obvious hard points on the floor were covered with foam, a more extensive treatment was impractical. Nevertheless, we are reasonably comfortable with the overall acoustic quality of the final configuration due to the weaker nature of these secondary reflections. In addition, the secondary reflections occur at delay times of approximately 25 msec

(around 1/4 revolution) and, therefore, are unlikely to contaminate the BVI pulses, which occur at intervals of 1/3 revolution.

The background noise due to a combination of wind noise over the microphones and tunnel drive noise was measured with the rotor hub spinning and all test hardware present except the rotor blades. Figure 9 shows the sound power spectra at Microphone #5 (obtained in the same manner as for rotor noise data described above) at several tunnel speeds. The high level peaks at the low frequencies arise from the tunnel drive fans. Figure 10 is a comparison of high BVI noise data at Microphone #5 to background noise at similar tunnel speeds. It can be seen that for this high BVI noise case, there is adequate signal-to-noise ratio within the frequency range of interest (300–1500 Hz) for BVI noise. Figure 11, on the other hand, shows a similar comparison for a relatively low BVI noise case. In this instance, it is apparent that the signal-to-noise is not adequate. It should be noted that although these comparisons are straightforward in the frequency domain, they cannot be easily done in the time domain because of lack of information regarding the relative phases of the rotor and the drive fans. Therefore, no attempt has been made to correct the time history data for background noise.

Data Files

Acoustic metrics (OASPL, DBA, and BLSPL) are presented in table 4 in Run/Point order. Contour plots of BLSPL levels under the forward advancing side (obtained from Mics #1-4 for the Runs/Points outlined in dark in table 3) are shown in figure 12. A range of operating conditions, as noted on the plots, near maximum BVI noise are provided. Note that in several cases these surveys were incomplete.

The complete set of acoustic data, including background noise data, is provided on a CD-ROM. The disk and file formats are described in the Appendix.

REFERENCES

1. Kitaplioglu, C; McCluer, M.; and Acree, Jr., C. W.: Comparison of XV-15 Full-Scale Wind Tunnel and In-Flight Blade-Vortex Interaction Noise. American Helicopter Society 53rd Annual Forum, Virginia Beach, VA, April 1997.
2. Light, J.: Results of an XV-15 Test in the National Full-Scale Aerodynamics Complex. American Helicopter Society 53rd Annual Forum, Virginia Beach, VA, April 1997.
3. Light, J.; Kitaplioglu, C.; and Acree, C. W.: XV-15 Aeroacoustic Testing at NASA Ames. 23rd European Rotorcraft Forum, Dresden, Germany, September 1997.
4. Maisel, M.: NASA/Army XV-15 Tilt Rotor Research Aircraft Familiarization Document. NASA TM X-62,407, January 1975.
5. Martin, R. M.; and Hardin, J. C.: Spectral Characteristics of Rotor Blade/Vortex Interaction Noise. Journal of Aircraft, vol. 25, no. 1, January 1988.

Table 1. XV-15 rotor characteristics

Blade number	3
Rotor radius	12.5 ft
Blade chord at tip	14 in
Rotor solidity	0.089
Blade twist	-41° (nonlinear)
Hub pre-cone angle	1.5°
Rotor airfoils	NACA 64-series

Table 2. Microphone positions

Mic #	x/R	y/R	z/R
1	variable	0.575	1.82
2	variable	0.752	1.82
3	variable	1.11	1.82
4	variable	1.46	1.82
5	4.87	2.82	2.05
6	3.6	-4.20	2.05

M _{tip}	RPM	C _T /σ	C _Q /σ	μ	α _{TPP}	X _m	RUN	POINT
0.691	590.9	0.0753	0.00358	0.125	1.95	37.5	9	23
0.691	591.3	0.0755	0.00357	0.125	1.96	75	9	22
0.691	591.1	0.0753	0.00357	0.125	1.95	112.5	9	21
0.690	590.7	0.0754	0.00358	0.125	1.94	150	9	20
0.691	591.3	0.0754	0.00358	0.125	1.95	187.5	9	19
0.690	591.1	0.0755	0.00359	0.125	1.95	225	9	18
0.689	590.2	0.0753	0.00359	0.125	1.95	262.5	9	17
0.691	591.1	0.0750	0.00358	0.125	1.92	300	9	16
0.689	590.0	0.0762	0.00349	0.125	2.95	225	9	28
0.691	591.4	0.0758	0.00338	0.125	3.96	-112.5	9	40
0.691	591.5	0.0762	0.00337	0.125	3.95	-75	9	39
0.690	591.0	0.0759	0.00339	0.125	3.95	-37.5	9	38
0.690	591.1	0.0762	0.00338	0.125	3.95	0	9	37
0.691	591.3	0.0761	0.00337	0.125	3.95	37.5	9	36
0.690	591.1	0.0761	0.00337	0.125	3.93	75	9	35
0.690	590.9	0.0760	0.00337	0.125	3.96	112.5	9	34
0.691	591.0	0.0756	0.00336	0.125	3.96	150	9	33
0.690	591.0	0.0760	0.00337	0.125	3.95	187.5	9	32
0.691	590.9	0.0761	0.00335	0.125	3.94	225	9	31
0.690	591.0	0.0763	0.00336	0.125	3.95	262.5	9	30
0.690	590.7	0.0760	0.00334	0.125	3.96	300	9	29
0.689	590.2	0.0761	0.00322	0.126	4.97	225	9	41
0.690	590.7	0.0756	0.00306	0.125	5.95	225	9	42
0.690	590.3	0.0756	0.00291	0.125	6.91	225	9	43
0.690	590.5	0.0754	0.00274	0.125	7.97	225	9	44
0.689	590.9	0.0765	0.00263	0.125	8.82	225	9	45
0.690	590.9	0.0756	0.00246	0.125	9.86	225	9	46
0.690	587.0	0.0757	0.00251	0.125	9.96	225	13	50
0.690	590.7	0.0755	0.00217	0.125	11.78	225	9	47
0.690	591.1	0.0765	0.00192	0.125	13.69	225	9	48
0.689	590.2	0.0763	0.00178	0.126	14.65	225	9	49
0.690	587.4	0.0755	0.00664	0.150	-15.04	225	13	47
0.690	587.8	0.0757	0.00646	0.150	-13.99	225	13	46
0.690	587.9	0.0757	0.00608	0.150	-11.96	225	13	45
0.691	588.2	0.0759	0.00572	0.150	-9.97	225	13	44
0.690	587.7	0.0755	0.00531	0.150	-8.00	225	13	43
0.690	583.7	0.0755	0.00485	0.151	-5.96	225	11	34
0.690	588.1	0.0727	0.00421	0.150	-3.71	0	13	25
0.690	587.8	0.0727	0.00421	0.150	-3.71	37.5	13	26
0.690	587.9	0.0726	0.00422	0.150	-3.71	75	13	27
0.690	587.7	0.0727	0.00422	0.150	-3.71	112.5	13	28
0.690	587.8	0.0728	0.00422	0.150	-3.70	150	13	29
0.690	587.7	0.0727	0.00423	0.150	-3.70	187.5	13	30
0.690	583.4	0.0759	0.00450	0.151	-4.01	225	11	33
0.690	587.8	0.0726	0.00423	0.150	-3.71	225	13	31
0.690	587.4	0.0725	0.00424	0.151	-3.72	262.5	13	32
0.690	587.5	0.0726	0.00424	0.150	-3.70	300	13	33
0.690	583.3	0.0758	0.00407	0.150	-1.91	225	11	32
0.690	582.6	0.0757	0.00385	0.150	-0.91	225	11	31
0.690	594.5	0.0754	0.00344	0.150	0.01	225	15	7
0.689	583.1	0.0759	0.00364	0.151	0.04	225	11	24
0.690	590.8	0.0757	0.00341	0.150	0.09	225	14	12
0.689	589.1	0.0760	0.00356	0.150	0.07	300	14	32
0.690	583.9	0.0758	0.00345	0.150	1.00	225	11	25
0.691	584.3	0.0757	0.00326	0.150	1.99	225	11	26
0.690	582.9	0.0758	0.00306	0.150	3.06	225	11	30
0.690	583.9	0.0756	0.00286	0.150	3.96	225	11	27
0.689	583.3	0.0759	0.00248	0.151	6.02	225	11	28
0.689	583.3	0.0759	0.00215	0.151	7.95	225	11	29
0.690	587.2	0.0758	0.00202	0.150	9.89	225	13	54
0.690	587.4	0.0759	0.00170	0.150	11.89	225	13	51
0.690	587.0	0.0756	0.00142	0.150	13.78	225	13	52

M _{tip}	RPM	C _T /σ	C _Q /σ	μ	α _{TPP}	X _m	RUN	POINT
0.690	585.2	0.0913	0.00355	0.170	3.09	262.5	12	84
0.690	585.3	0.0912	0.00355	0.170	3.09	300	12	85
0.689	584.7	0.0909	0.00331	0.170	4.02	225	12	86
0.690	585.3	0.0914	0.00307	0.170	5.01	225	12	87
0.689	584.7	0.0910	0.00345	0.181	3.08	225	12	90
0.690	595.5	0.0998	0.00441	0.148	3.07	225	15	33
0.690	590.5	0.0964	0.00554	0.157	-2.92	225	14	28
0.690	590.3	0.0964	0.00496	0.157	-0.90	225	14	24
0.690	589.5	0.1006	0.00499	0.157	0.10	225	14	22
0.691	591.0	0.0964	0.00440	0.156	1.03	225	14	19
0.690	590.1	0.1044	0.00499	0.156	1.07	225	14	20
0.690	594.9	0.1022	0.00459	0.156	1.28	225	15	13
0.690	594.9	0.1013	0.00462	0.156	1.55	225	15	14
0.690	591.0	0.0990	0.00439	0.157	1.55	225	14	17
0.691	595.2	0.0957	0.00427	0.156	1.55	225	15	16
0.690	594.7	0.1035	0.00477	0.156	1.59	225	15	15
0.690	590.9	0.1034	0.00437	0.157	2.61	225	14	16
0.690	594.6	0.1025	0.00407	0.156	2.96	225	15	8
0.690	594.2	0.0964	0.00381	0.156	3.11	225	15	11
0.690	595.8	0.1016	0.00423	0.159	3.14	225	15	32
0.690	594.6	0.1010	0.00406	0.156	3.15	225	15	9
0.691	588.7	0.0970	0.00326	0.156	5.54	225	13	14
0.690	596.0	0.0991	0.00446	0.170	1.03	225	15	30
0.689	594.5	0.1023	0.00435	0.171	2.06	225	15	29
0.690	596.0	0.1022	0.00407	0.171	3.09	225	15	34
0.690	595.3	0.1017	0.00392	0.180	3.06	225	15	31
0.690	590.9	0.1068	0.00497	0.157	1.63	225	14	18
0.690	594.1	0.1068	0.00445	0.157	3.22	225	15	10
0.690	591.0	0.1077	0.00439	0.157	3.53	225	14	15
0.690	595.7	0.1061	0.00428	0.170	3.06	0	15	28
0.690	595.3	0.1054	0.00428	0.170	3.06	37.5	15	27
0.690	594.6	0.1058	0.00426	0.170	3.06	75	15	26
0.690	594.7	0.1058	0.00427	0.171	3.06	112.5	15	25
0.689	594.6	0.1057	0.00427	0.170	3.05	150	15	24
0.689	594.6	0.1056	0.00426	0.171	3.07	187.5	15	23
0.690	595.2	0.1056	0.00425	0.170	3.06	225	15	22
0.690	595.1	0.1055	0.00422	0.170	3.06	262.5	15	21
0.690	595.4	0.1055	0.00423	0.170	3.07	300	15	20
0.690	594.5	0.1049	0.00388	0.170	4.04	225	15	19
0.690	594.7	0.1054	0.00358	0.170	5.03	225	15	18
0.690	590.5	0.1124	0.00439	0.157	4.61	225	14	14
0.690	590.5	0.1118	0.00398	0.157	5.60	225	14	13

Run	Point	Mic#1- OASPL DBA	Mic#2- OASPL DBA	Mic#3- OASPL DBA	Mic#4- OASPL DBA	Mic#5- OASPL DBA	Mic#6- OASPL DBA
9	6.9	117.7	107.05	108.8	112.94	102.16	103.59
9	7.0	116.55	102.37	103.34	111.7	97.57	98.17
9	7.1	115.56	98.71	100.91	110.58	94.21	95.96
9	7.1	119.14	111.47	115.71	120.03	112.55	111.57
11	11	119.64	111.75	116.19	120.57	117.12	120.84
11	13	120.01	111.33	115.74	120.84	112.64	117.04
11	14	119.44	109.69	114.57	120.87	112.29	116.46
11	15	119.28	108.07	111.91	120.18	109.08	120.28
11	16	119.58	110.31	114.6	120.5	111.37	115.47
11	17	116.16	106.81	109.25	116.06	108.71	115.62
11	18	117.49	111.16	114.12	117.07	110.31	113.19
11	19	118.61	111.18	115.18	119.27	115.92	115.64
11	20	118.09	111.09	114.5	119.3	111.13	114.4
11	21	117.75	111.19	113.95	117.32	110.25	112.65
11	22	117.22	111.33	118.33	121.32	112.32	119.32
11	23	117.83	111.34	109.43	112.47	118.04	109.16
11	24	118.23	109.25	113.19	118.34	109.31	113.16
11	25	118.94	109.91	114.13	119.16	110.42	114.61
11	26	119.75	110.93	115.28	120.15	111.7	116.07
11	27	118.95	110.06	114.2	119.73	111.14	115.34
11	28	118.33	108.44	112.32	119.32	113.18	116.95
11	29	117.49	111.16	114.12	117.07	110.35	113.19
11	30	119.68	110.97	115.3	120.31	111.92	116.3
11	31	117.94	109.66	113.38	117.92	109.37	112.91
11	32	117.61	111.21	113.66	116.87	109.66	112.83
11	33	117.22	111.33	114.35	116.79	110.58	113.43
11	34	115	106.49	108.74	114.8	106.51	108.25
12	12	120.55	112.86	116.75	120.98	113.6	117.45
12	13	120.88	113.17	117.29	121.46	114.09	118.12
12	14	120.92	113.25	117.67	121.3	113.73	117.8
12	15	121.47	114.16	118.31	121.53	113.93	118.2
12	16	121.11	113.04	117.17	121.64	113.52	117.82
12	17	120.46	111.73	114.79	121.45	112.92	116.13
12	18	120.22	111.42	114.52	121.22	115.26	120.91
12	19	120.17	110.84	113.52	120.88	111.88	116.42
12	20	119.79	109.98	112.24	120.59	112.07	114.45
12	21	120.93	111.4	113.87	121.71	113.44	116.3
12	22	121.24	112.06	114.5	122.03	113.44	116.4
12	23	121.05	111.75	114.55	122.29	113.27	116.74
12	24	121.09	111.98	115.4	122.18	113.4	117.44
12	25	121.71	113.31	117.26	122.25	113.83	118.18
26/27	12	121.95	114.36	118.42	121.99	114.11	118.28
12	28	121.54	113.74	118.13	121.81	114.06	118.34
12	29	121.13	113.14	117.25	121.73	114.02	118.1
12	30	120.8	112.27	116.55	121.31	113.55	117.44
12	31	120.93	112.58	115.63	121.47	113.55	117.16
12	32	121.48	113.34	117.16	122.03	114.26	118.08
12	33	121.84	114.01	118.14	122.13	114.29	118.27
12	34	122.43	114.77	118.84	122.39	114.49	118.63
12	35	122.33	114.13	117.79	122.93	114.77	118.96
12	36	121.88	112.94	115.97	123.02	114.4	122.47
12	37	121.83	112.82	115.61	123.05	114.62	118.18
12	38	122.36	113.53	116.61	123.07	114.94	118.51
12	39	121.49	112.17	115.31	122.35	114.29	117.52
12	40	120.87	111.47	114.53	121.76	113.47	121.5
12	41	121.77	112.84	115.83	122.37	114.17	117.35
12	42	121.73	112.78	114.4	122.78	114.34	118.34

Run	Point	Mic#1-	Mic#2-	Mic#3-	Mic#4-	Mic#5-	Mic#6-
		OASPL	DBA	BLSPL	OASPL	DBA	BLSPL
12	44	121.76	113.08	116.17	122.82	118.24	122.61
12	45	122.19	114.07	117.74	122.85	114.82	118.99
12	46	122.27	114.59	118.32	122.23	118.38	122.4
12	47	121.68	113.76	117.78	122.09	114.42	118.11
12	48	121.35	113.07	116.64	121.99	114.2	117.75
12	49	120.8	112.19	115.54	121.36	113.22	116.71
12	50	120.37	110.7	114.03	120.97	115.42	121.18
12	51	120.88	111.78	115.42	121.5	116.68	121.34
12	52	121.2	112.78	116.77	121.66	113.3	121.68
12	53	121.81	113.37	117.6	121.8	113.73	117.84
12	54	121.8	113.61	117.41	122.44	114.38	118.6
12	55	121.33	112.54	115.59	122.07	114.06	117.78
12	56	121.11	111.89	115.37	121.93	113.38	117.48
12	57	121.05	111.79	115.12	121.65	113.09	116.93
12	58	120.14	109.91	112.92	120.94	111.71	114.86
12	59	121.94	112.3	115.14	123.07	114.75	118.1
12	60	122.23	112.89	112.89	123.08	114.39	115.77
12	61	122.11	112.95	115.68	123.07	114.24	117.49
12	62	122.2	113.43	116.23	123.2	114.76	117.9
12	63	122.73	114.58	118.32	123.22	115.24	119.22
12	64	122.62	114.78	118.96	122.58	114.63	122.45
12	65	122.1	113.82	117.89	122.47	114.42	118.24
12	66	121.75	113.21	117.33	122.3	114.2	118.26
12	67	121.33	112.67	116.48	121.88	113.7	121.78
12	68	119.99	111.77	114.99	120.48	112.57	115.98
12	69	120.57	112.44	116.05	121.25	113.3	116.89
12	70	121.11	113.23	117.38	121.31	113.45	117.56
12	71	121.85	114.28	118.32	121.72	113.98	118.36
12	72	121.79	113.75	117.42	122.37	114.42	118.69
12	73	121.57	113.04	116.15	122.59	114.62	118.49
12	74	121.52	113.22	116.47	122.67	115.08	118.8
12	75	121.42	113.3	116.48	121.56	113.76	117.25
12	76	119.59	109.89	112.53	120	111.03	114.44
12	77	121.26	112.6	114.63	122.16	117.1	121.16
12	78	121.64	113.33	115.45	122.42	114.73	117.15
12	79	121.28	112.88	114.83	122.49	114.42	116.87
12	80	121.2	112.89	116.09	122.35	114.33	117.93
12	81	121.5	113.35	117.09	122.21	114.29	118.27
12	82	121.87	114.47	118.53	121.79	114.17	121.23
12	83	121.23	113.38	117.79	121.58	113.82	118.2
12	84	120.94	113.11	117.2	121.54	114	118.11
12	85	120.53	112.55	116.37	120.97	113.28	117.17
12	86	121.29	113.31	117.67	121.62	117.99	121.57
12	87	121.42	113.35	117.3	121.87	113.99	117.72
12	88	120.46	112.8	117.25	120.68	113.04	117.41
12	89	119.96	112.69	117.05	120.13	112.95	117.13
12	90	121.94	113.32	118.21	122.19	114.17	120.57
12	91	120.83	112.91	117.09	120.77	112.97	117.01
12	92	120.48	112.13	115.81	120.33	112.15	115.86
12	93	120.02	109.55	112.68	120.18	109.71	113.2
12	94	120.42	110.14	113.46	120.86	110.71	114.22
12	95	120.66	110.7	114.48	120.91	110.69	114.62
12	96	121.05	111.93	115.38	120.93	111.1	115.07
12	97	120.86	111.17	113.88	121.59	112.11	115.7
12	98	120.73	110.9	113.47	121.57	112.2	115.34
12	99	120.77	111.33	113.85	121.67	113.09	116.62
12	100	120.93	112.23	115.57	121.67	114.11	117.65

	Point	Mic#1 - OASPL	Mic#2 - OASPL	Mic#3 - OASPL	Mic#4 - OASPL	Mic#5 - OASPL	Mic#6 - OASPL
Run		DBA	DBA	DBA	DBA	DBA	DBA
12	101	119.98	110.76	114.43	121.06	113.44	117.27
12	102	120.12	109.63	113.28	120.41	109.72	113.58
12	103	119.85	109.26	112.67	120.15	109.19	112.9
12	104	120.37	110.69	114.76	120.61	110.64	114.69
12	105	120.38	111.49	115.58	120.64	111.47	115.56
12	106	121.37	112.42	116.37	121.77	112.84	116.77
12	107	119.44	109.53	112.87	119.74	109.3	112.95
12	108	118.07	109.25	112.53	118.34	109.28	112.83
13	14	119.86	110.64	114.43	119.75	110.71	114.58
13	15	119.19	109.64	113.88	119.34	109.94	114.13
13	16	118.12	111.21	114.58	117.66	110.85	114.96
13	17	118.23	111.38	114.96	117.1	110.9	114.25
13	18	117.77	110.8	114.54	117.19	110.23	113.66
13	19	117.59	110.77	114.56	116.8	109.58	113.21
13	20	116.99	109.77	113.68	116.43	108.86	112.54
13	21	115.74	107.93	111.37	115.61	107.44	110.73
13	22	114.62	105.97	109.75	114.47	105.46	109.22
13	23	113.36	103.79	107.32	113	103.53	106.7
13	24	111.51	101.27	104.11	111.48	101.25	104.1
13	25	110.65	100.26	102.85	110.9	100.19	102.41
13	26	112.7	103.76	106.68	112.33	102.79	105.32
13	27	114.12	106.31	109.46	113.62	105.08	108.78
13	28	115.08	108.08	110.08	114.53	106.71	109.38
13	29	116.05	109.62	112.52	115.31	108.29	110.86
13	30	116.71	110.54	113.38	115.69	108.78	111.31
13	31	116.9	110.34	113.21	116.1	109.22	111.65
13	32	117.28	110.63	113.36	116.4	109.27	111.6
13	33	117.23	110.55	113.14	116.33	109.11	111.4
13	34	115.47	103.79	106.15	114.86	102.97	105.03
13	35	115.55	103.89	106.46	115.04	103.12	105.32
13	36	115.14	103.33	105.89	115.47	102.82	104.97
13	37	114.82	103.49	105.75	114.45	102.64	104.64
13	38	114.5	102.62	104.55	114.23	101.92	103.59
13	39	113.7	100.99	102.43	113.58	104.49	104.47
13	40	112.86	99.98	101.37	112.79	99.33	100.44
13	41	112.17	98.19	99.34	112.15	98.01	99.43
13	42	110.65	96.13	97.27	110.76	96.49	98.64
13	43	113.65	100.6	101.88	113.09	100.37	101.24
13	44	112.65	95.52	96.07	111.98	95.06	94.49
13	45	112.1	94.41	93.52	111.33	94.21	93.7
13	46	111.6	94.33	94.88	110.75	94.12	94.55
13	47	111.28	93.99	94.95	110.49	93.61	94.3
13	48	109.12	89.2	85.99	107.97	88.96	86.03
13	49	109.57	90.59	88.36	108.53	90.22	88.1
13	50	117.53	109.17	112.19	117.43	108.98	112.03
13	51	116.17	103.29	105.25	116.44	102.63	104.15
13	52	115.35	99.88	101.93	115.68	100.06	102.3
13	53	114.82	97.89	99.7	115.17	98.17	99.85
13	54	117.07	107.08	110.87	117.27	106.62	110.18
14	12	118.35	109.31	112.95	118.36	109.32	112.78
14	13	119.64	110.26	113.44	119.7	110.54	113.64
14	14	119.64	110.78	113.88	119.53	110.78	113.76
14	15	119.86	111.39	114.87	119.66	111.34	114.71
14	16	119.53	111.03	114.84	119.27	110.91	114.62
14	17	118.86	110.4	114.6	118.67	110.46	114.52
14	18	118.61	109.9	113.75	118.3	109.73	113.48
14	19	118.68	110.42	114.61	118.54	110.57	114.71

Run	Point	Mic#1-	Mic#2-	Mic#3-	Mic#4-	Mic#5-	Mic#6-
		OASPL	DBA	BLSPL	OASPL	DBA	BLSPL
14	20	118.3	109.66	113.67	118.08	109.67	113.47
14	21	118.52	110.59	114.78	118.48	110.89	114.78
14	22	118.1	109.94	113.92	117.99	110.11	117.99
14	23	118.49	111.13	115.16	118.38	111.27	114.98
14	24	118.05	110.5	114.53	117.95	110.71	114.46
14	25	118.42	111.95	115.67	118.18	111.79	115.26
14	26	117.93	110.87	114.85	117.71	110.88	114.55
14	27	117.42	110.73	114.4	117.12	110.58	114.56
14	28	117.07	109.59	113.38	116.86	109.63	113.12
14	29	116.54	109.43	112.66	116.15	109.09	112.01
14	30	116.06	107.96	111.45	115.79	107.91	111.07
14	31	115.08	105.82	108.8	114.8	105.68	108.33
15	6	99.03	86.32	86.14	98.43	85.85	87.04
15	7	118.23	109.22	112.71	118.13	109.18	112.46
15	8	119.94	111.58	115.1	119.76	111.63	115.13
15	9	120.1	111.89	115.56	119.92	111.93	115.59
15	10	119.62	111.12	114.42	119.3	110.98	114.29
15	11	120.44	112.35	116.17	120.32	112.47	116.08
15	12	120.81	113.04	116.94	120.77	113.25	117.07
15	13	118.76	109.97	113.99	118.45	109.82	113.78
15	14	118.87	110.41	114.43	118.35	110.35	114.22
15	15	118.78	110.19	114.16	118.46	110.08	114.95
15	16	119.04	110.7	114.84	118.87	110.82	114.84
15	17	119.3	111.26	115.36	119.21	111.45	115.38
15	18	120.62	112.59	116.72	121.05	112.34	116.74
15	19	120.63	112.74	116.88	120.89	113.16	117.32
15	20	119.65	111.9	115.47	119.87	112.26	115.87
15	21	119.86	112.15	116.07	120.31	112.91	116.07
15	22	119.89	112.22	116.39	120.1	112.52	116.78
15	23	120.24	112.89	116.76	120.17	112.52	116.46
15	24	119.87	112.06	115.76	120.43	112.57	116.69
15	25	119.28	110.33	113.76	120.3	112.28	115.6
15	26	119.21	110.81	113.16	120.18	111.8	114.19
15	27	118.73	109.73	111.03	119.5	110.78	112.59
15	28	118.84	109.23	110.36	119.53	110.24	110.66
15	29	119.49	111.9	116.24	119.55	112.06	119.35
15	30	119.34	112.21	116.28	119.42	112.55	116.44
15	31	120.78	112.94	117.14	121.1	113.24	117.5
15	32	120.02	111.93	115.67	119.83	111.98	115.68
15	33	119.58	111.23	114.33	119.41	111.25	114.22
15	34	120.26	112.52	116.61	120.52	112.92	117.05
15	35	118.9	108.07	110.87	119.57	108.73	111.53
15	36	117.68	105.75	109.44	118.21	106.35	109.69
15	37	116.61	102.83	106.41	117.12	103.02	106.38
15	38	116.35	100	102.87	116.85	100.86	102.88
15	39	115.51	104.28	105.74	115.17	103.99	104.93
15	40	114.61	99.32	99.15	114.23	98.41	99.13
15	41	114.07	101.58	102.72	113.65	101.24	102.22
15	42	113.31	100.96	102.08	112.78	100.28	101.24
15	43	113.05	95.9	96.03	112.5	95.54	95.58



Figure 1. The XV-15 right-hand rotor mounted in the Ames 80- by 120-Foot Wind Tunnel.

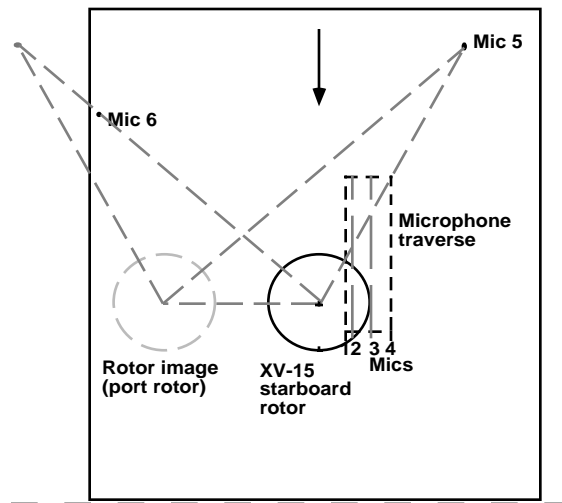


Figure 2. Schematic of microphone positions for the XV-15 test in the NASA Ames 80- by 120-Foot Wind Tunnel.

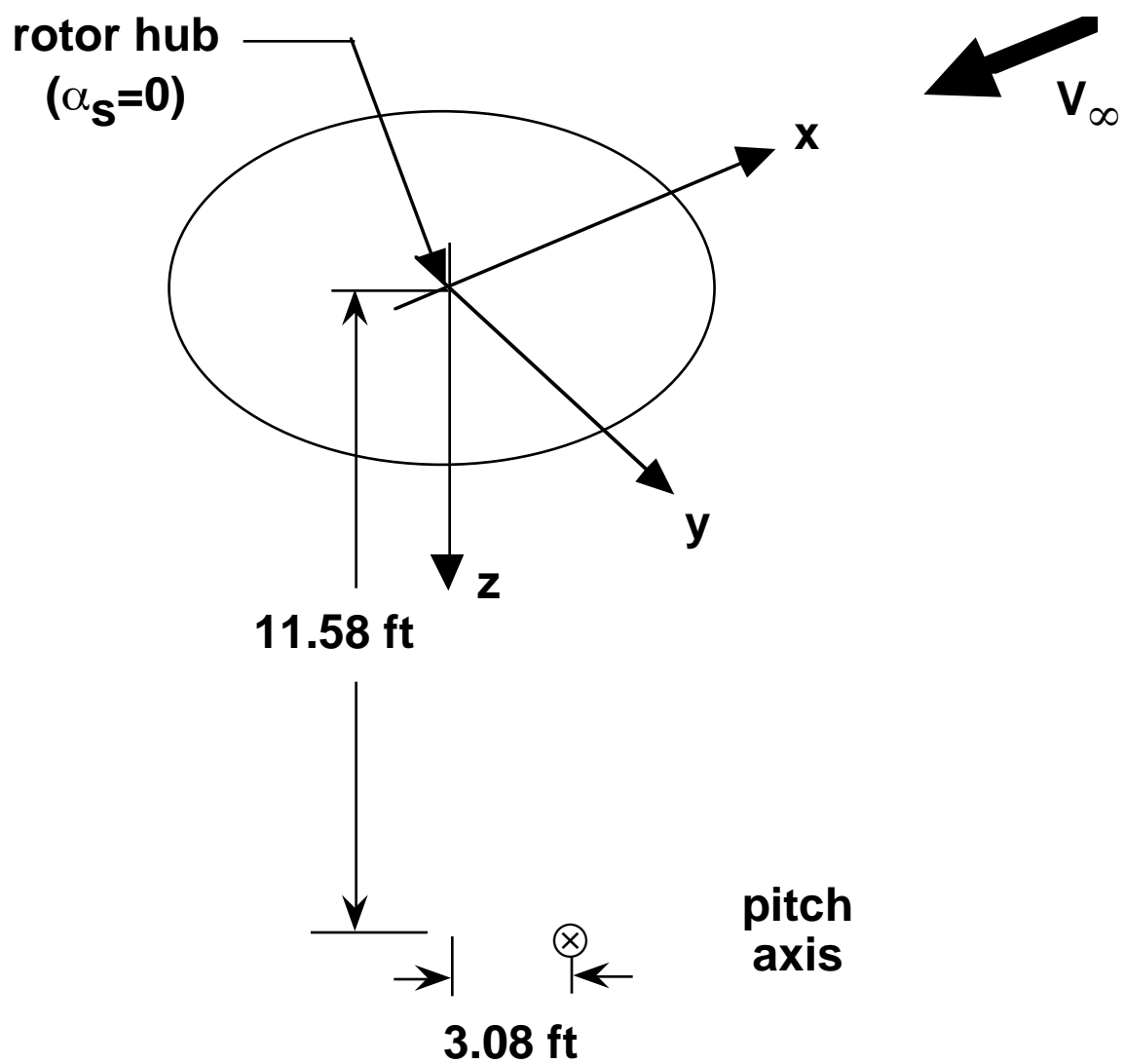


Figure 3. Coordinate system.

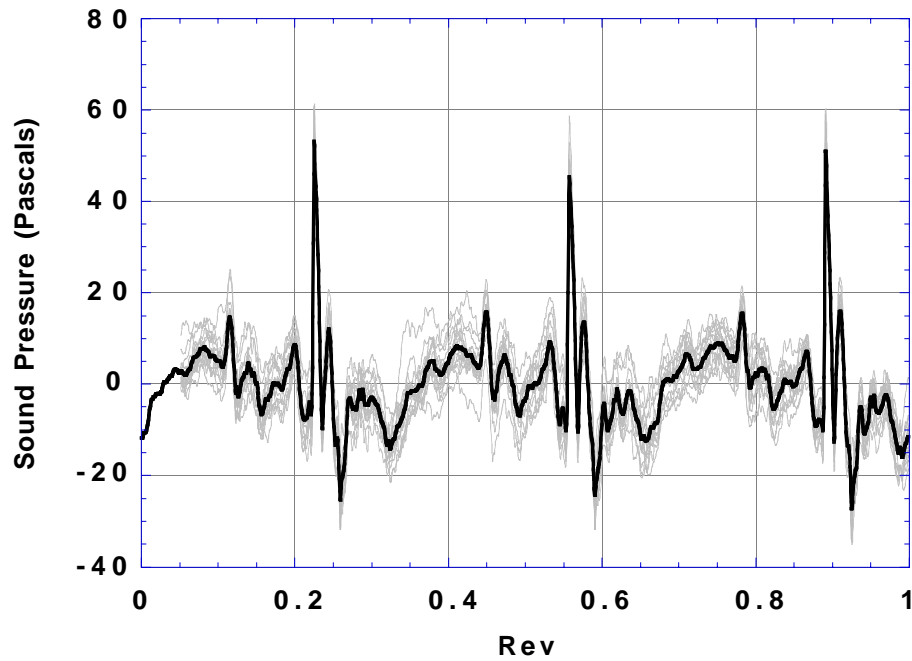


Figure 4(a). Comparing individual revs (light lines) to the average (dark line).

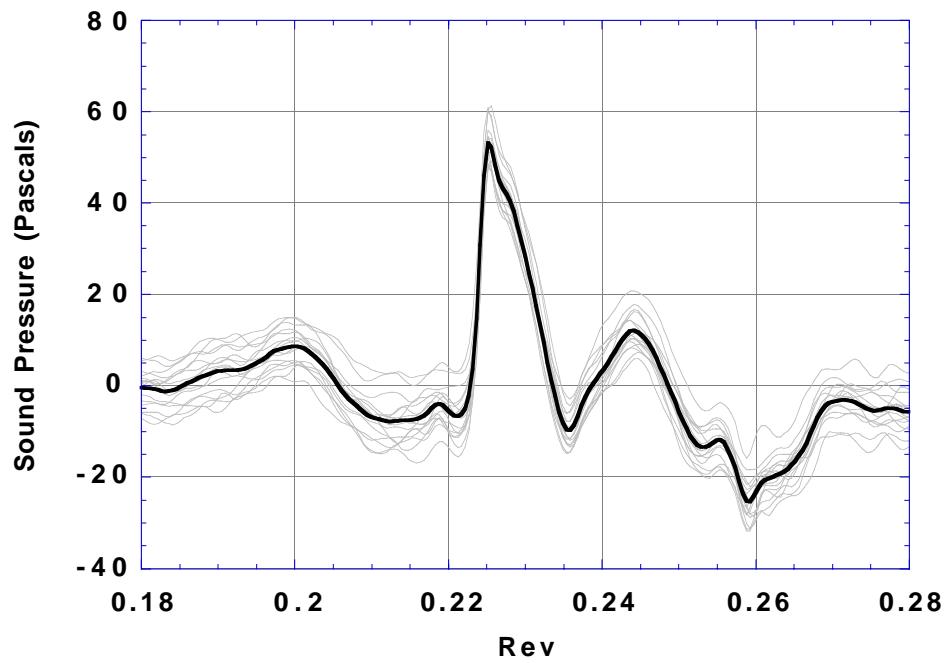


Figure 4(b). Expanded azimuth near the first BVI pulse.

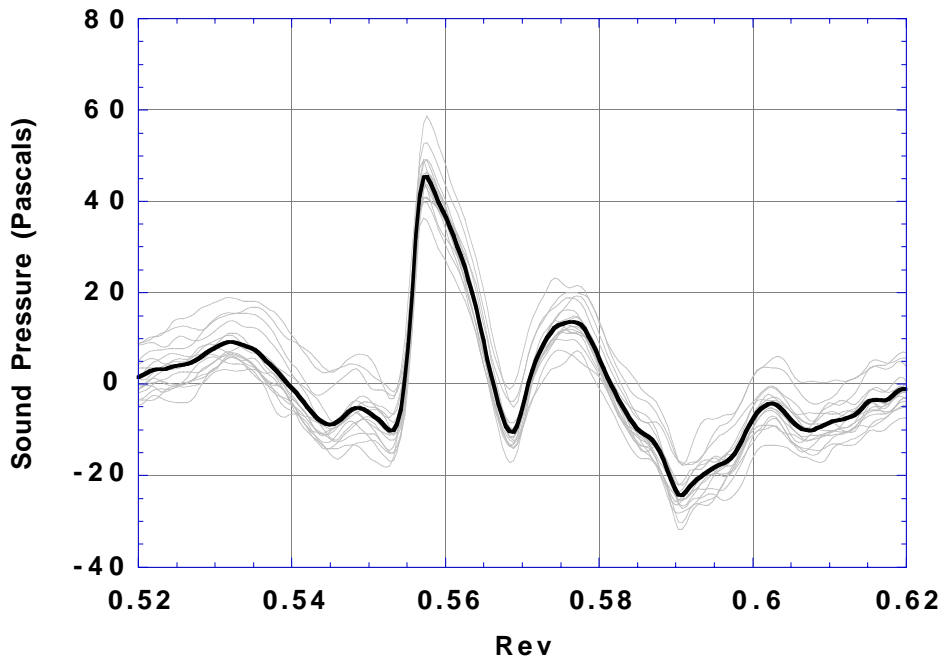


Figure 4(c). Expanded azimuth near the second BVI pulse.

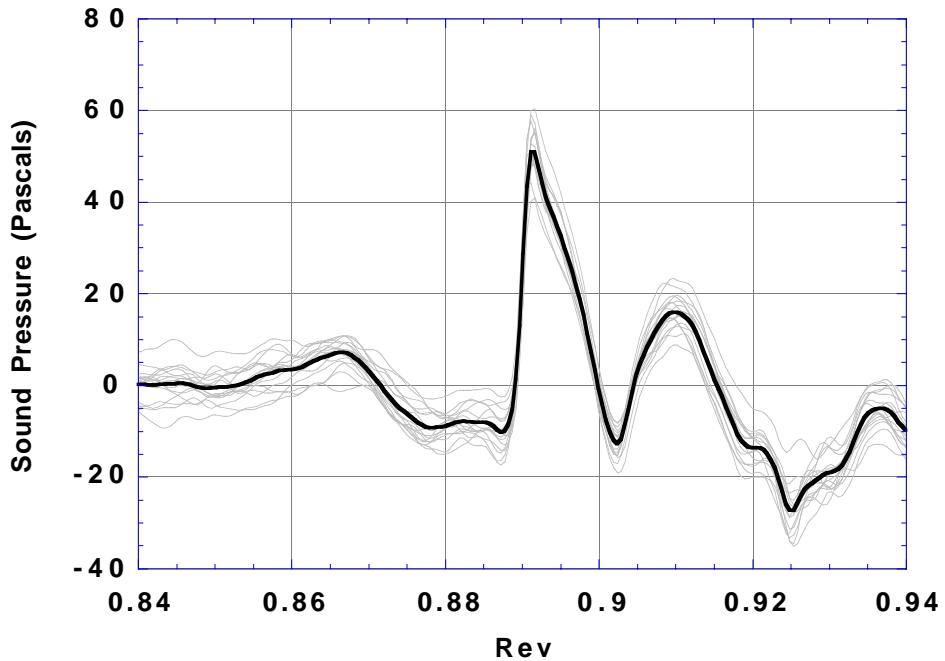


Figure 4(d). Expanded azimuth near the third BVI pulse.

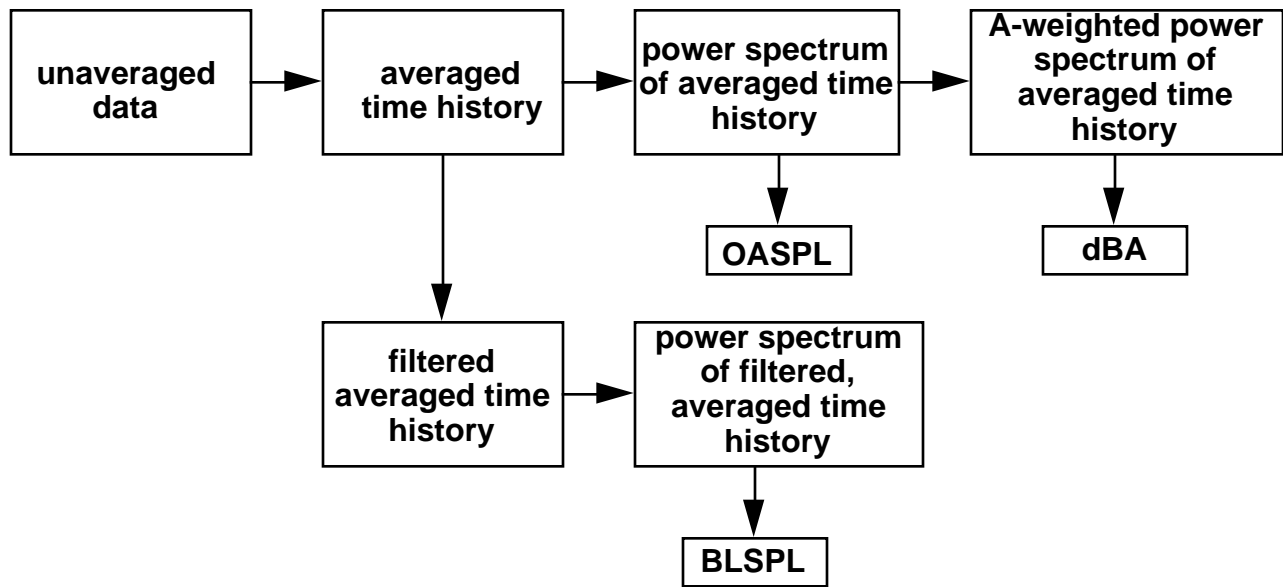


Figure 5. Data processing procedure.

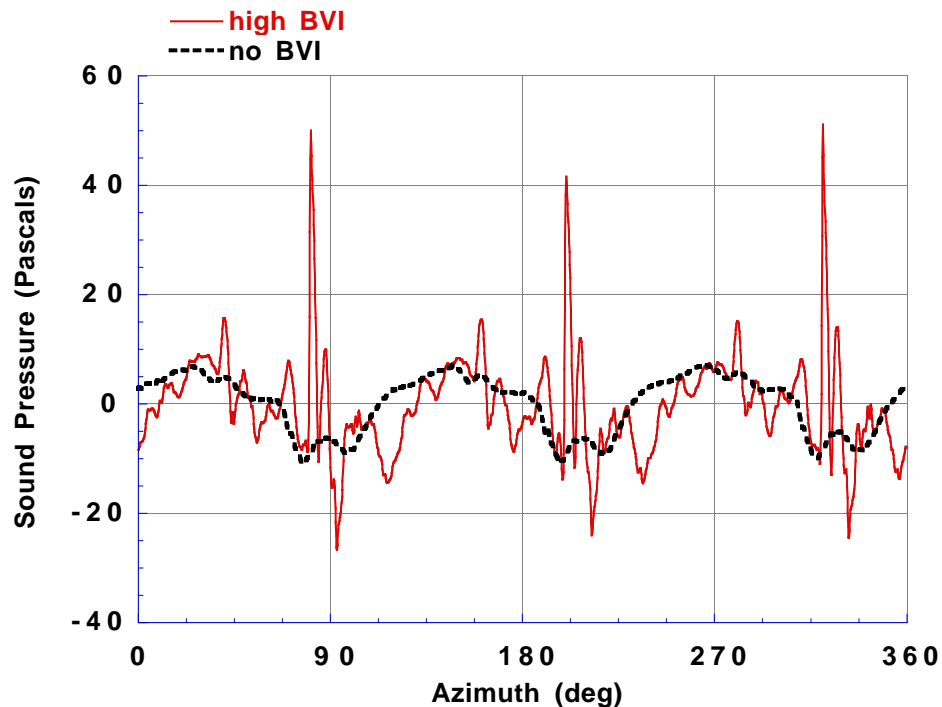


Figure 6. Comparison of a high BVI noise case with a case where no BVI noise is present, Microphone #5. Unfiltered data.

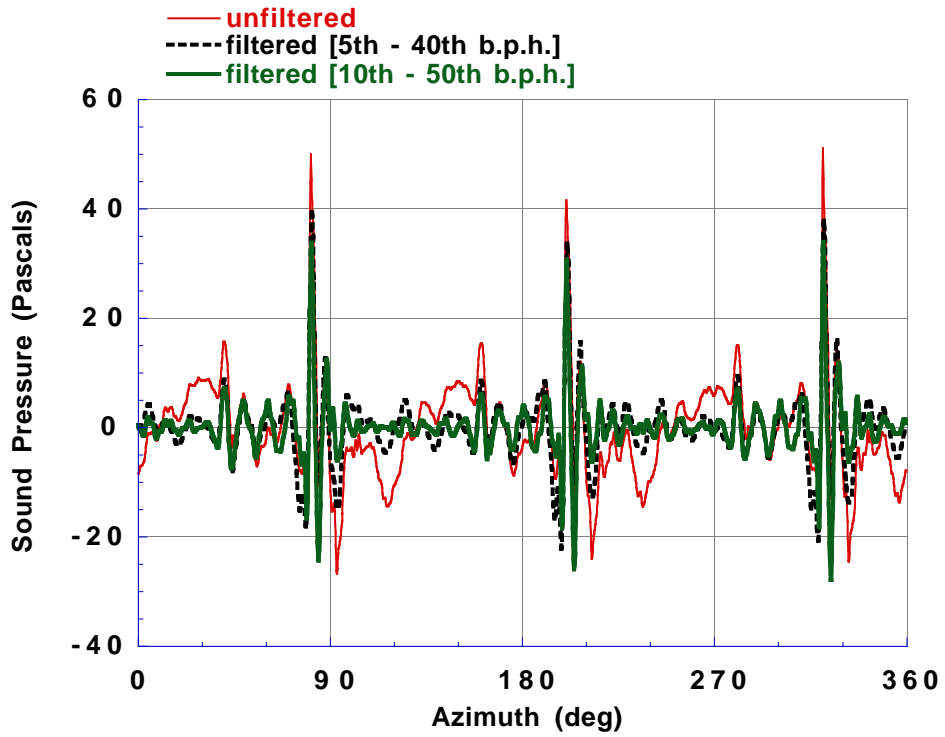


Figure 7(a). Comparison of unfiltered data with data filtered at two bandpass frequencies.

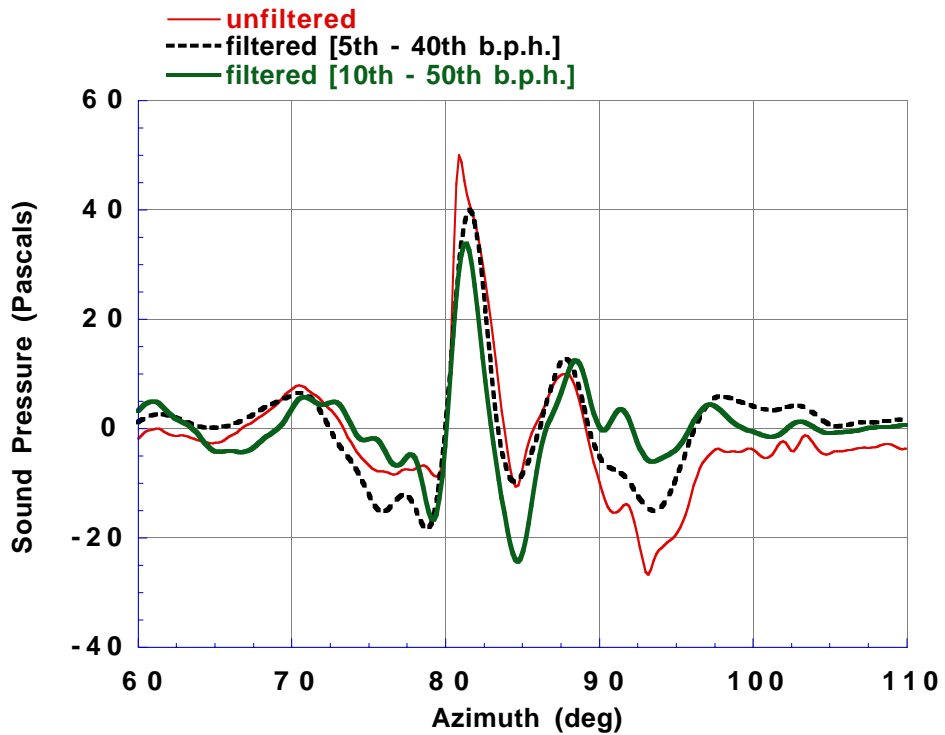


Figure 7(b). Expanded azimuth scale.

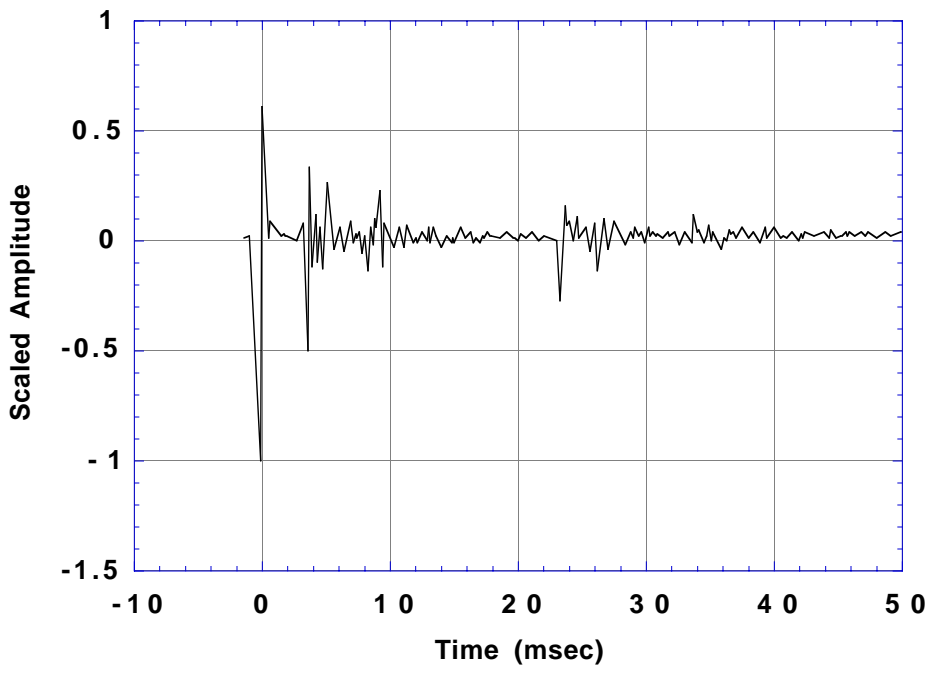


Figure 8(a). Reflection data without foam treatment, Mic #5.

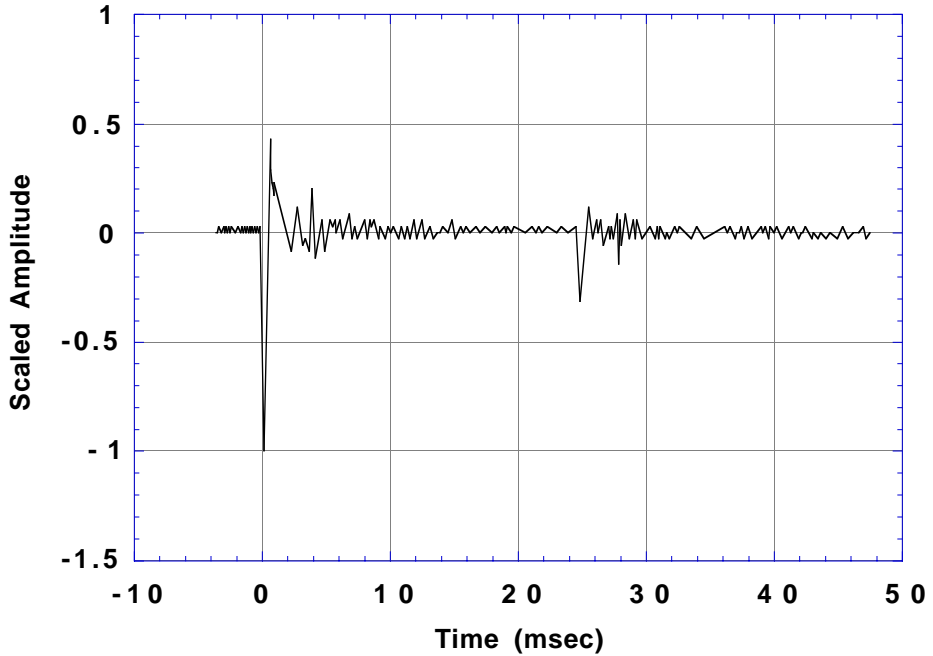


Figure 8(b). Reflection data after adding foam treatment.

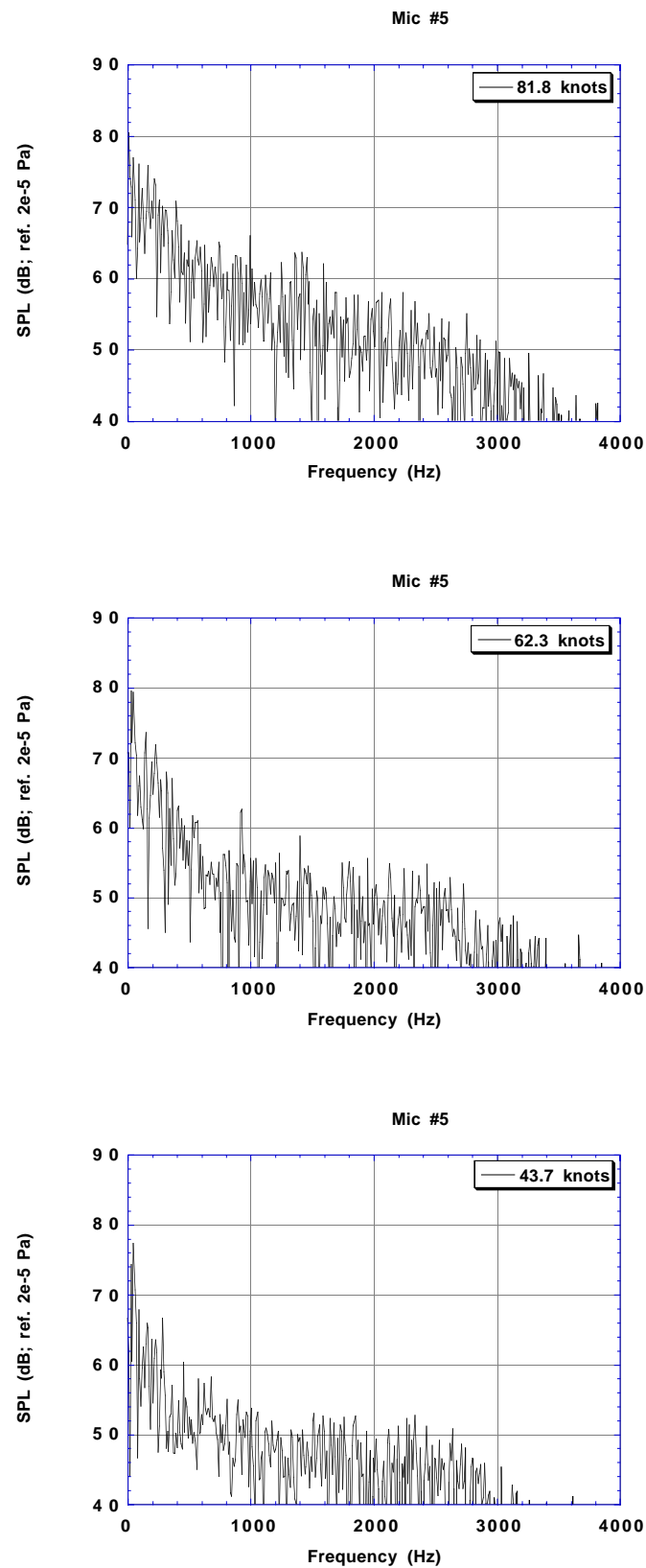


Figure 9. Power spectra of background noise at several tunnel speeds.

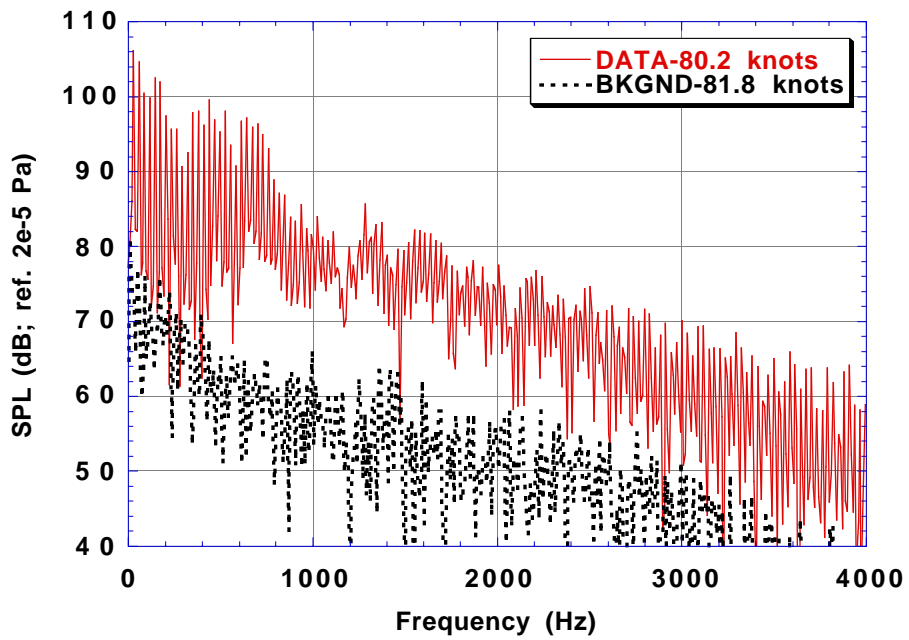


Figure 10. Comparison of data to background noise at a high BVI noise condition.

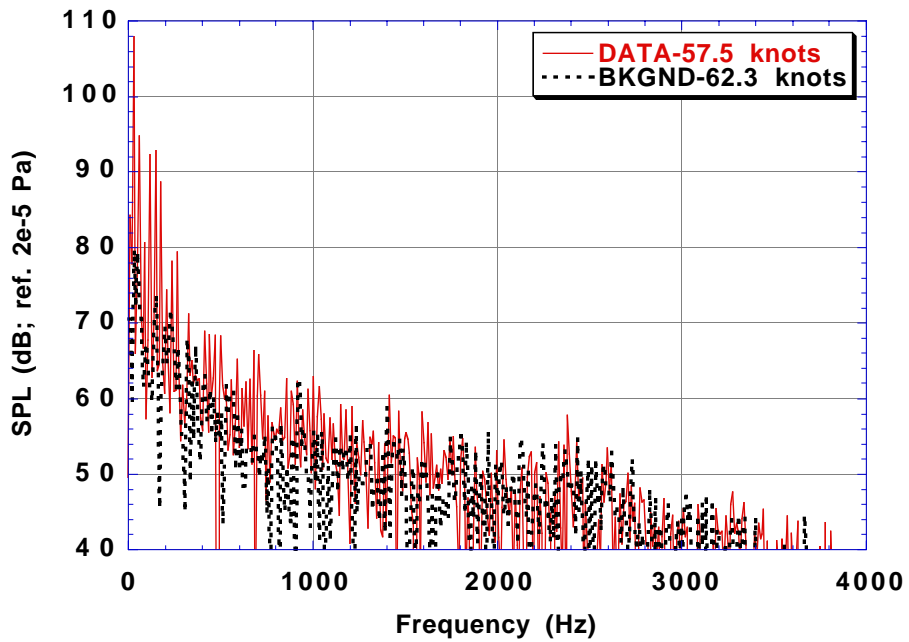


Figure 11. Comparison of data to background noise at a low BVI noise condition.

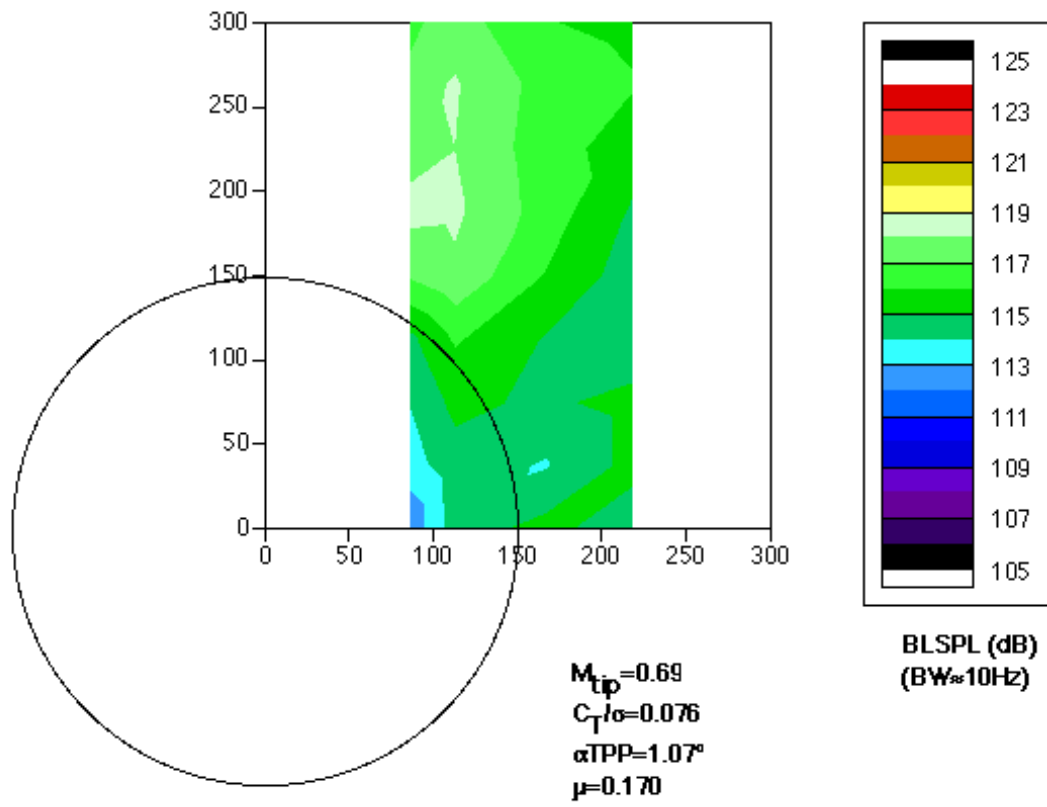


Fig 12. Contour plots of Band Limited Sound Pressure Level (BLSPL) under the forward advancing side of the starboard XV-15 rotor at operating conditions near maximum BVI noise.

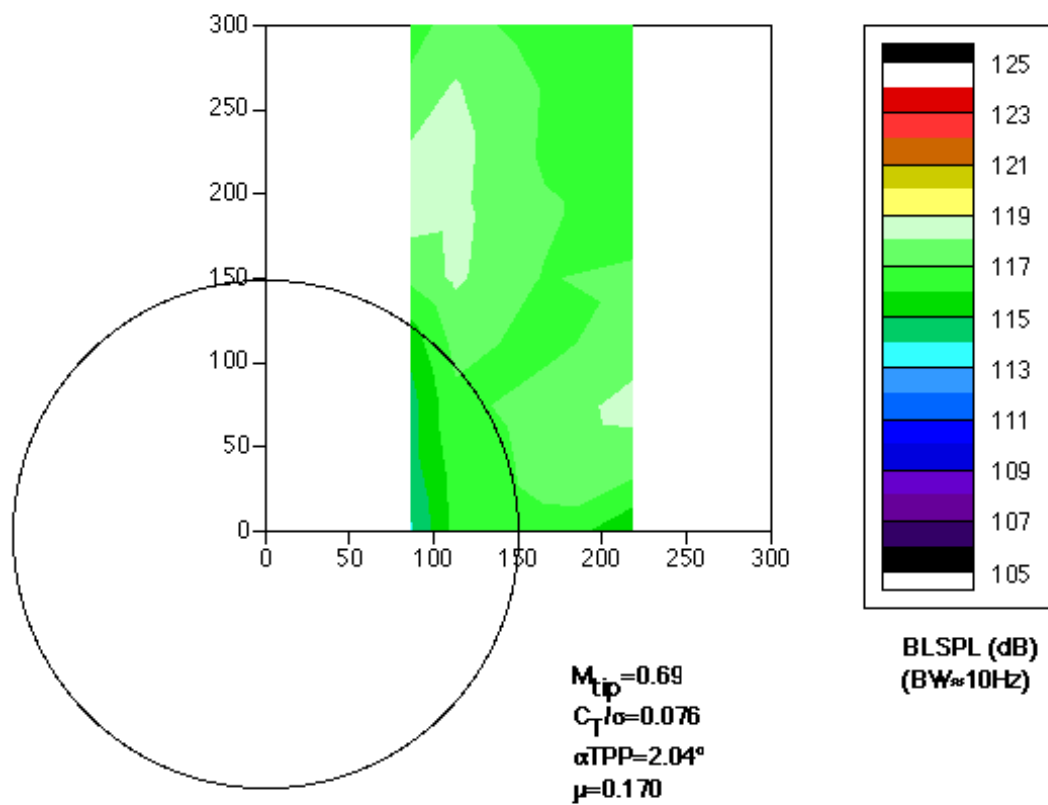


Fig 12. Continued.

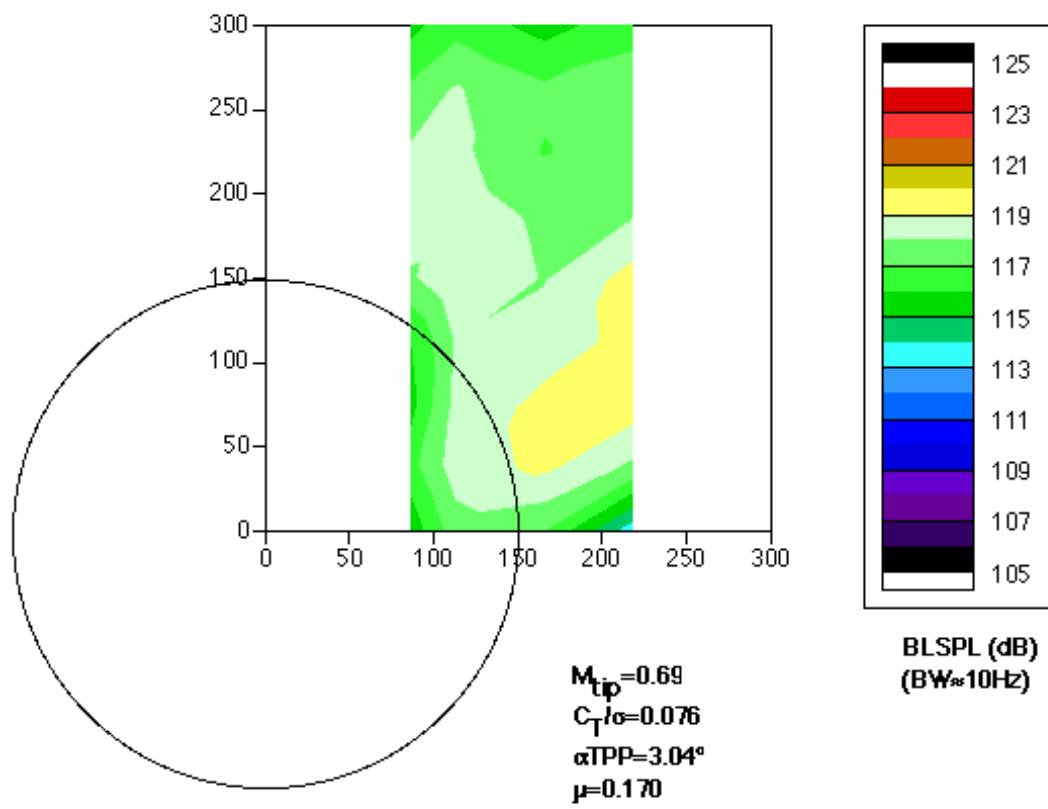


Fig 12. Continued.

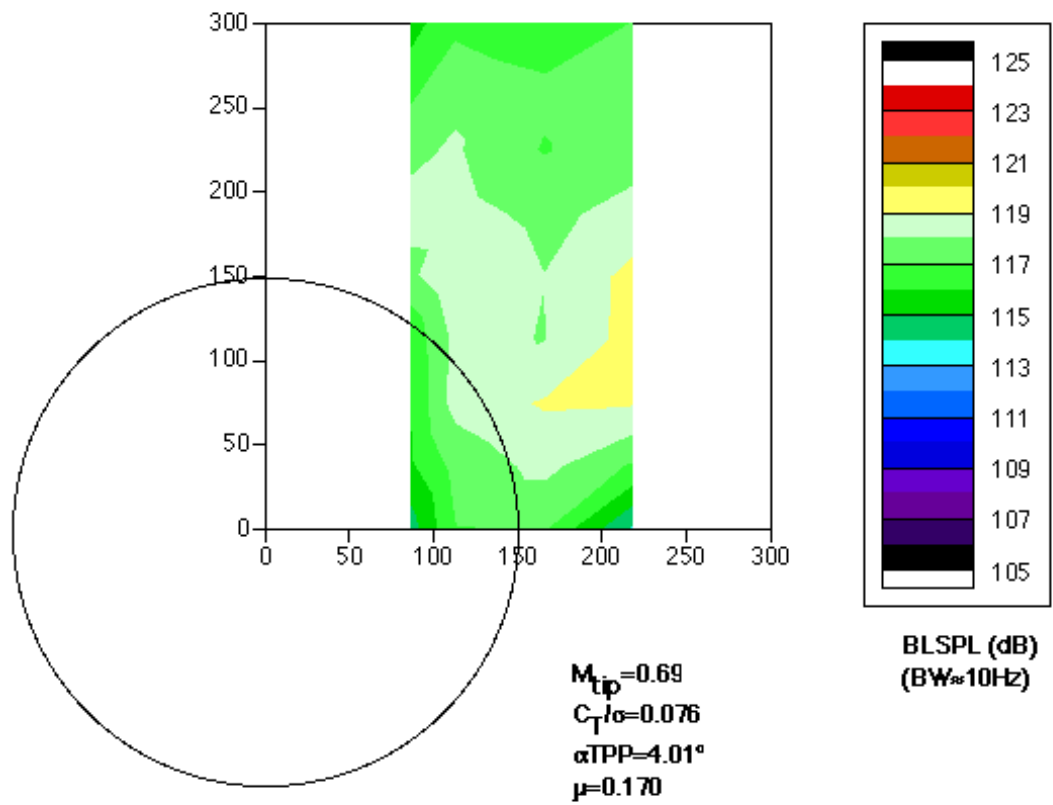


Fig 12. Continued.

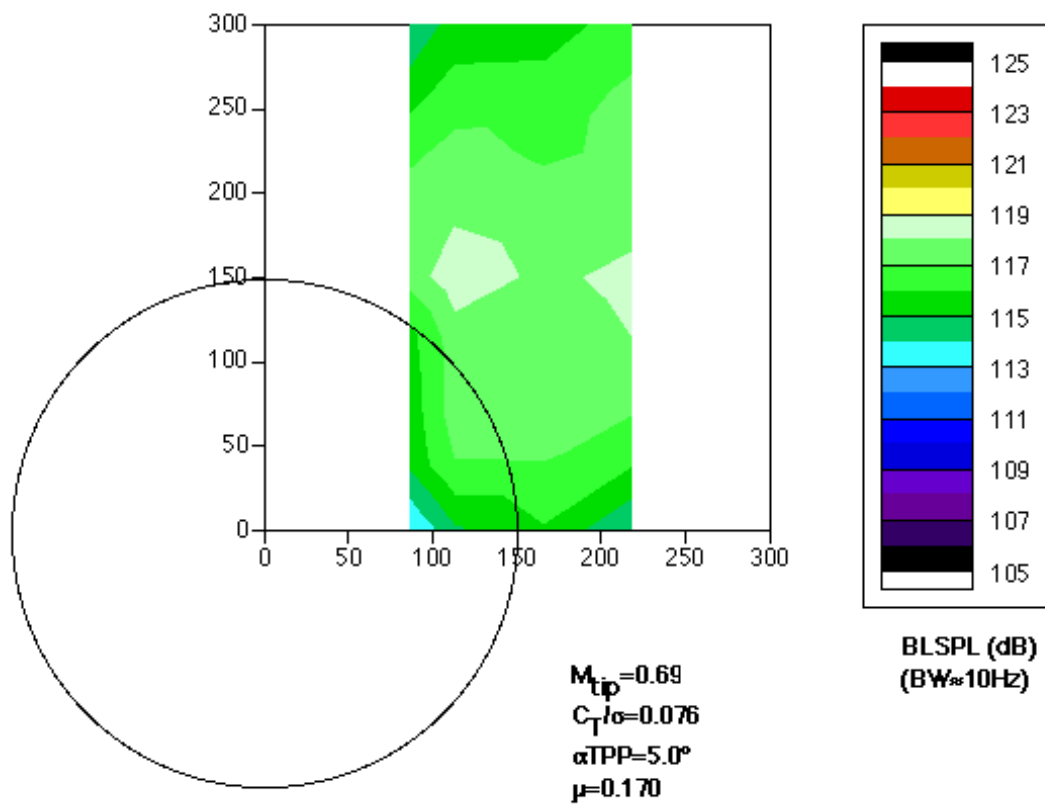


Fig 12. Continued.

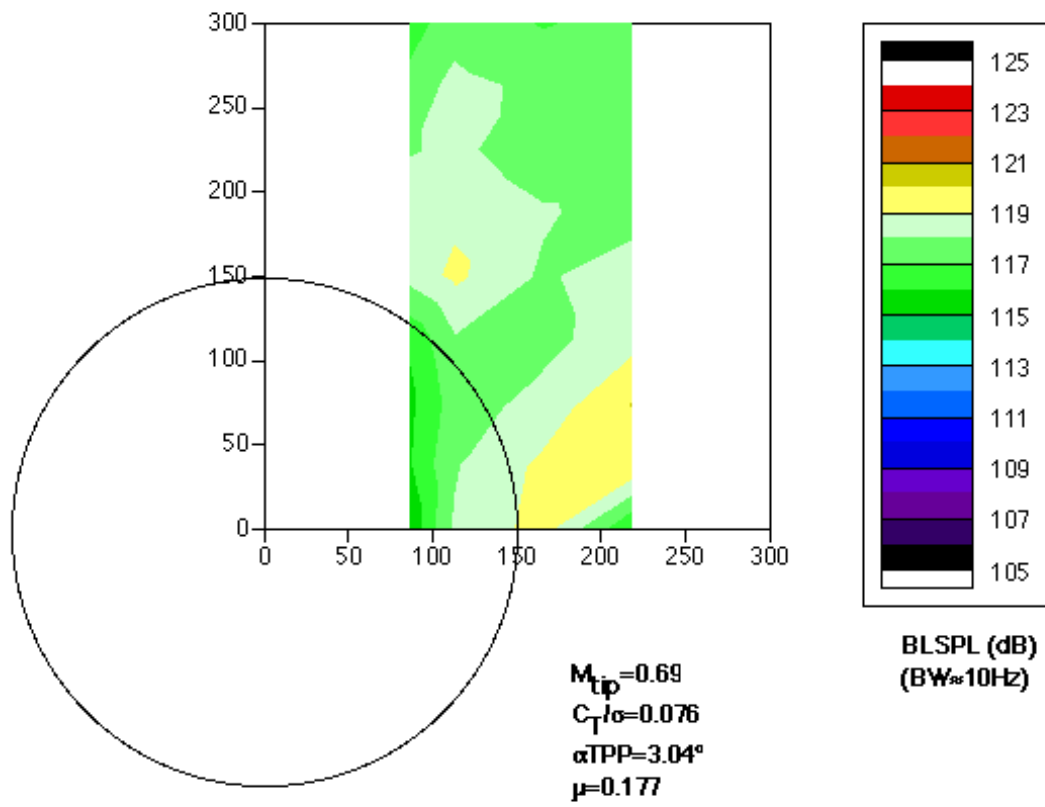


Fig 12. Continued.

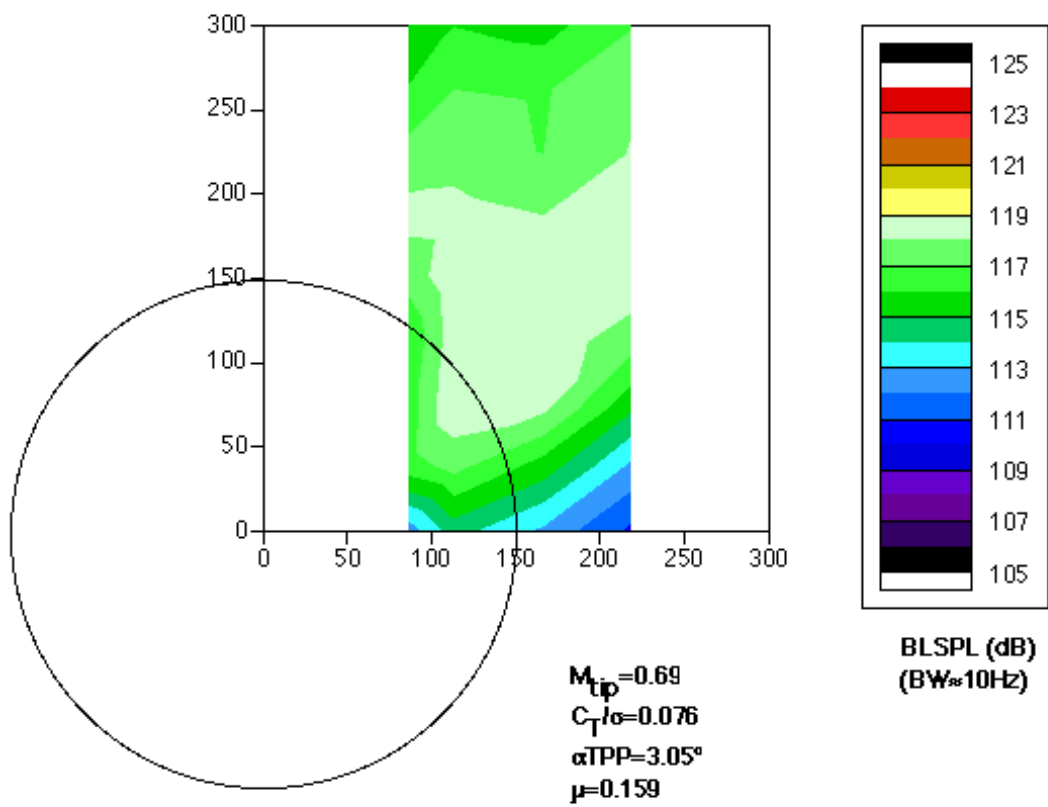


Fig 12. Continued.

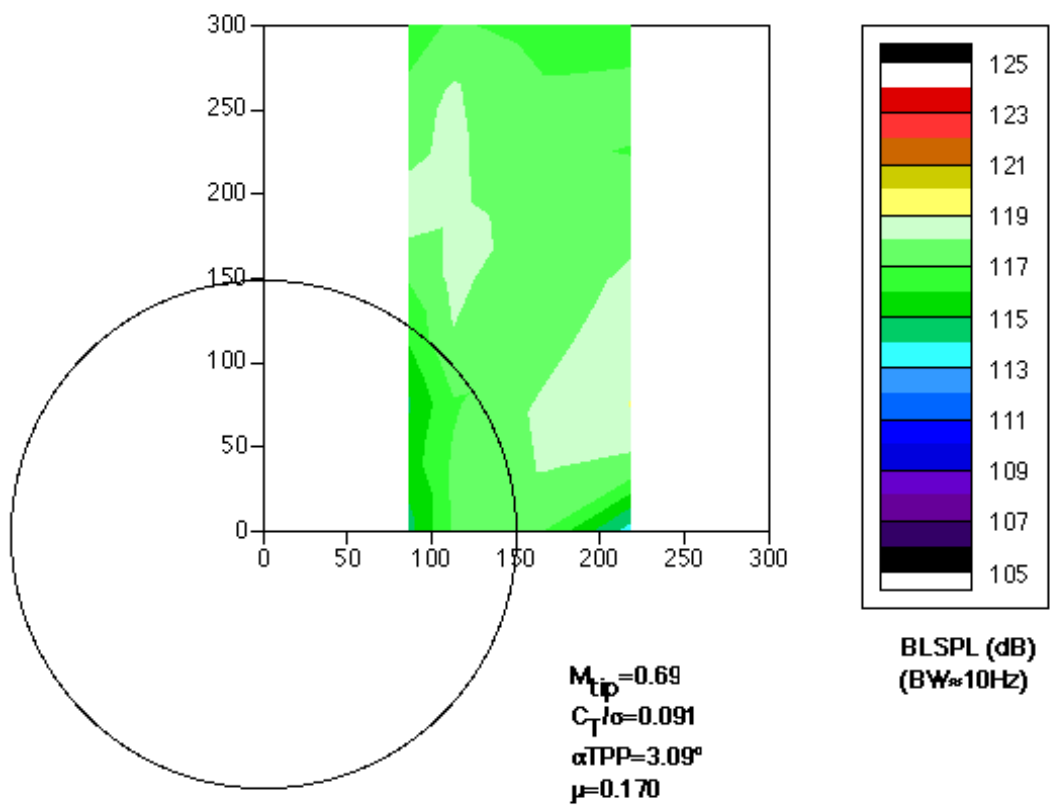


Fig 12. Continued.

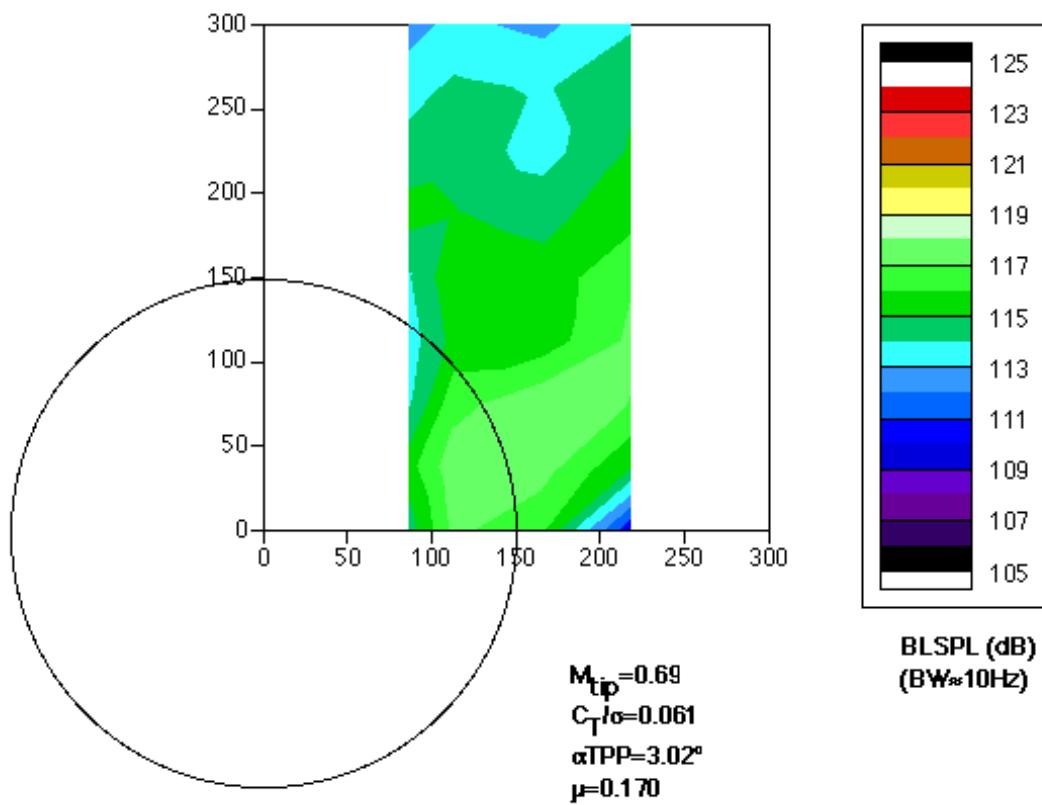


Fig 12. Continued.

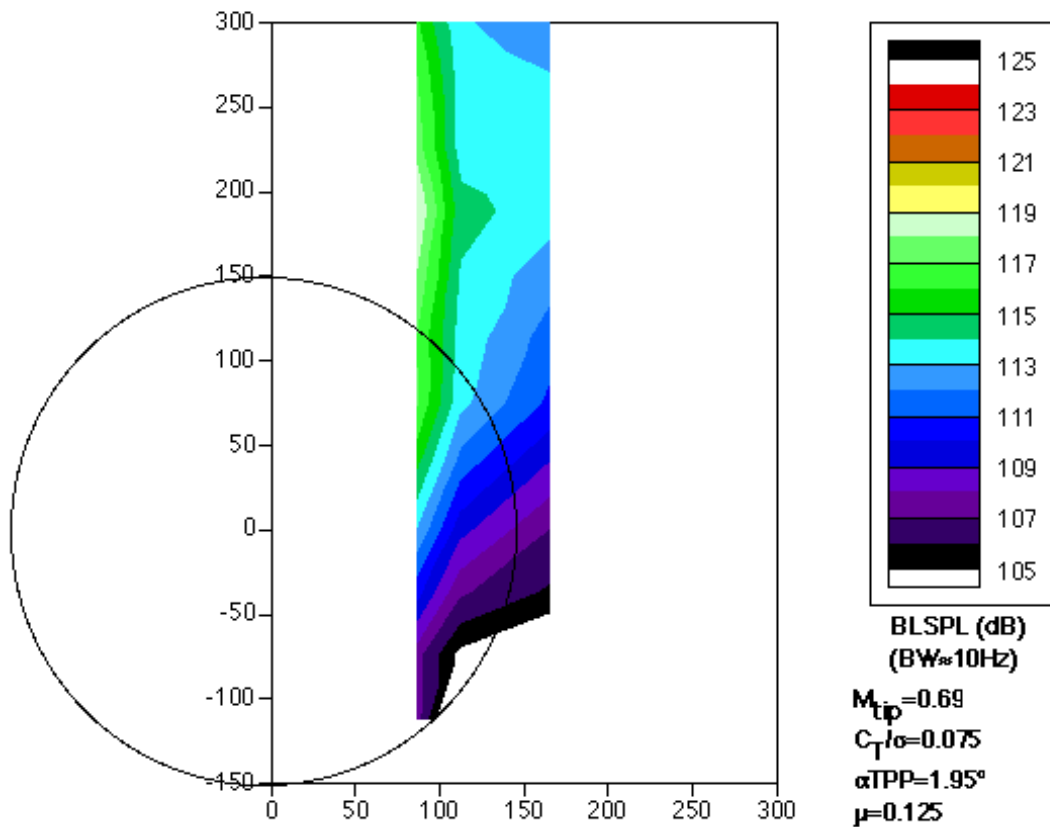


Fig 12. Continued.

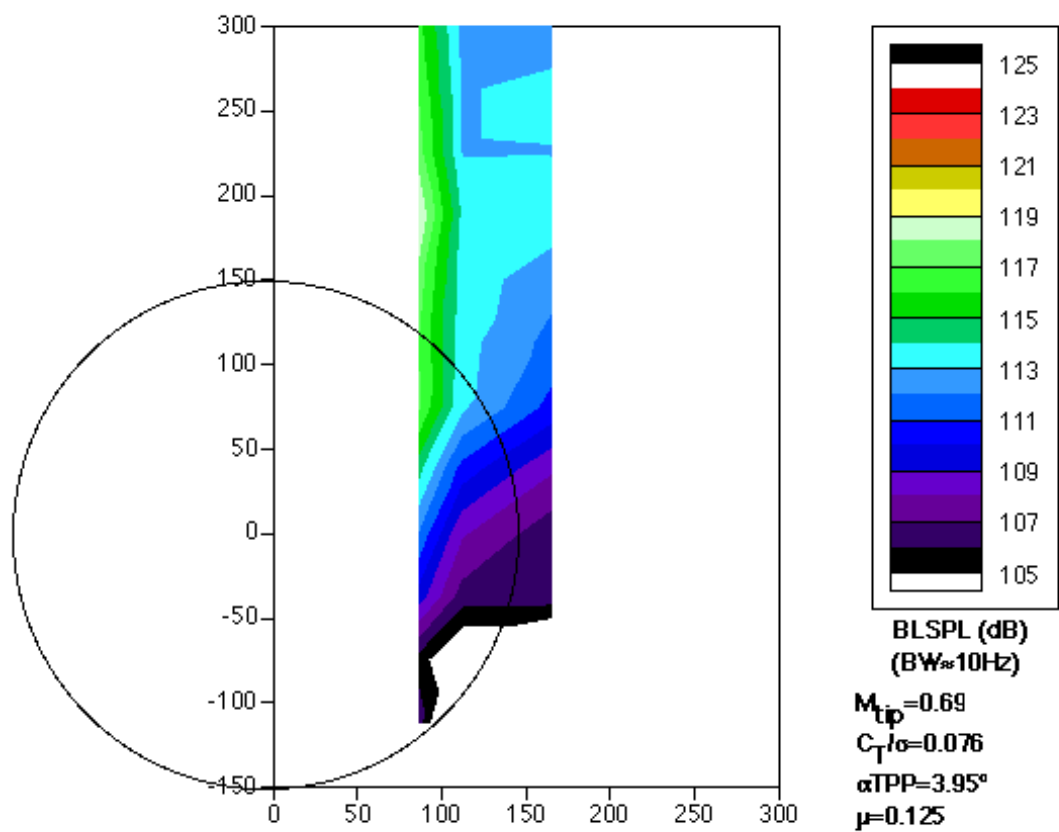


Fig 12. Continued.

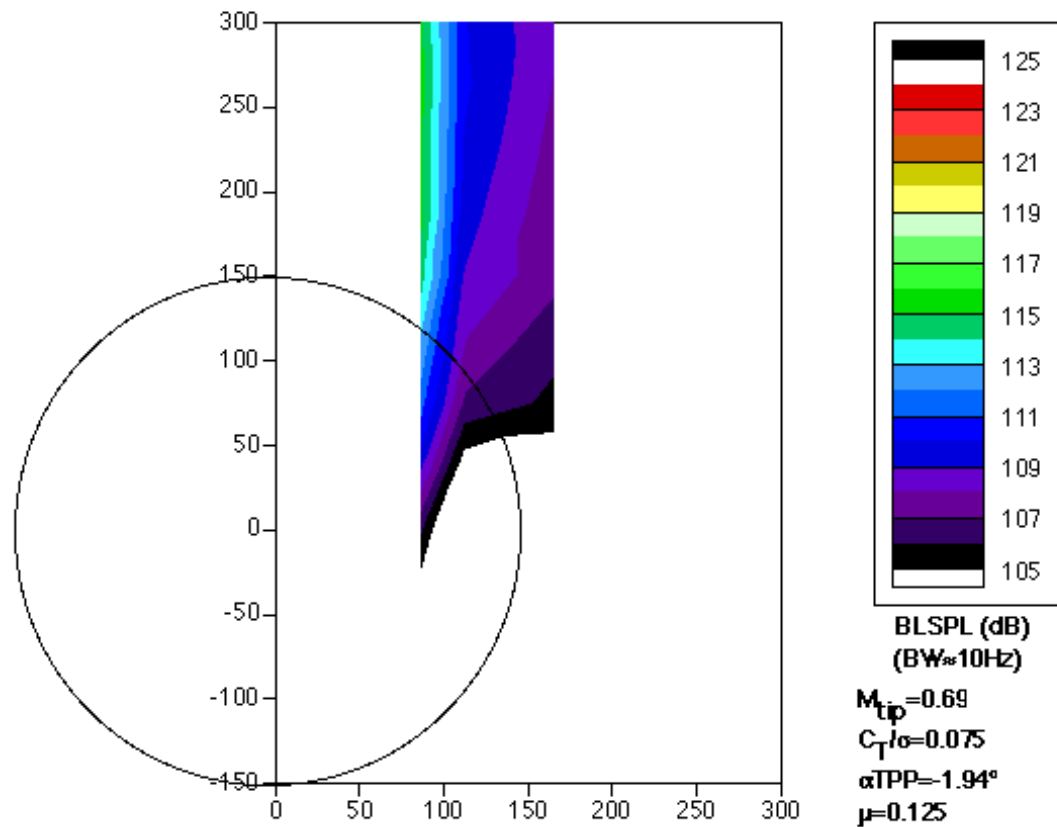


Fig 12. Continued.

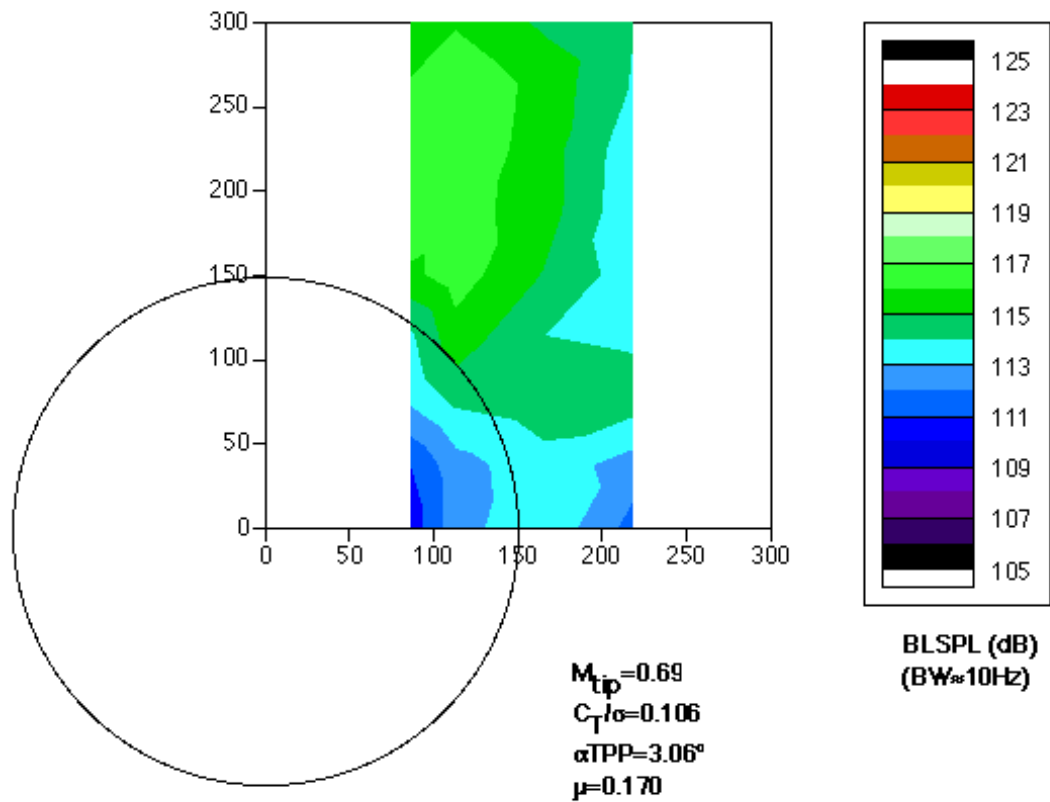


Fig 12. Continued.

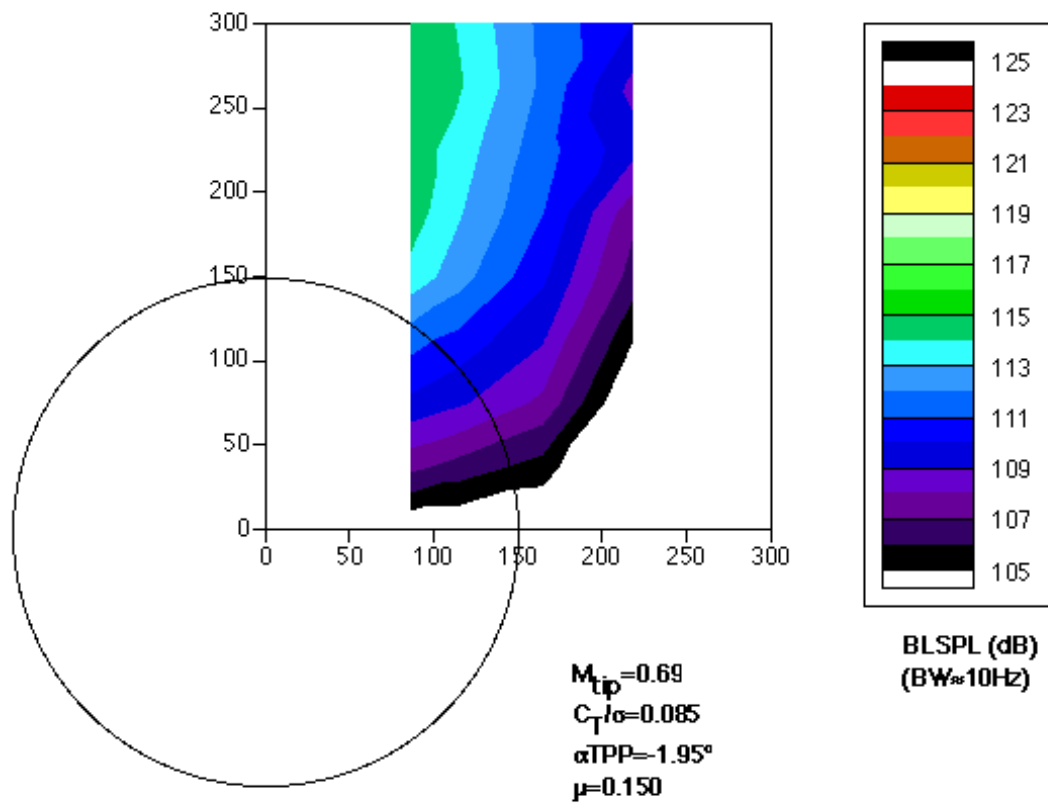


Fig 12. Continued.

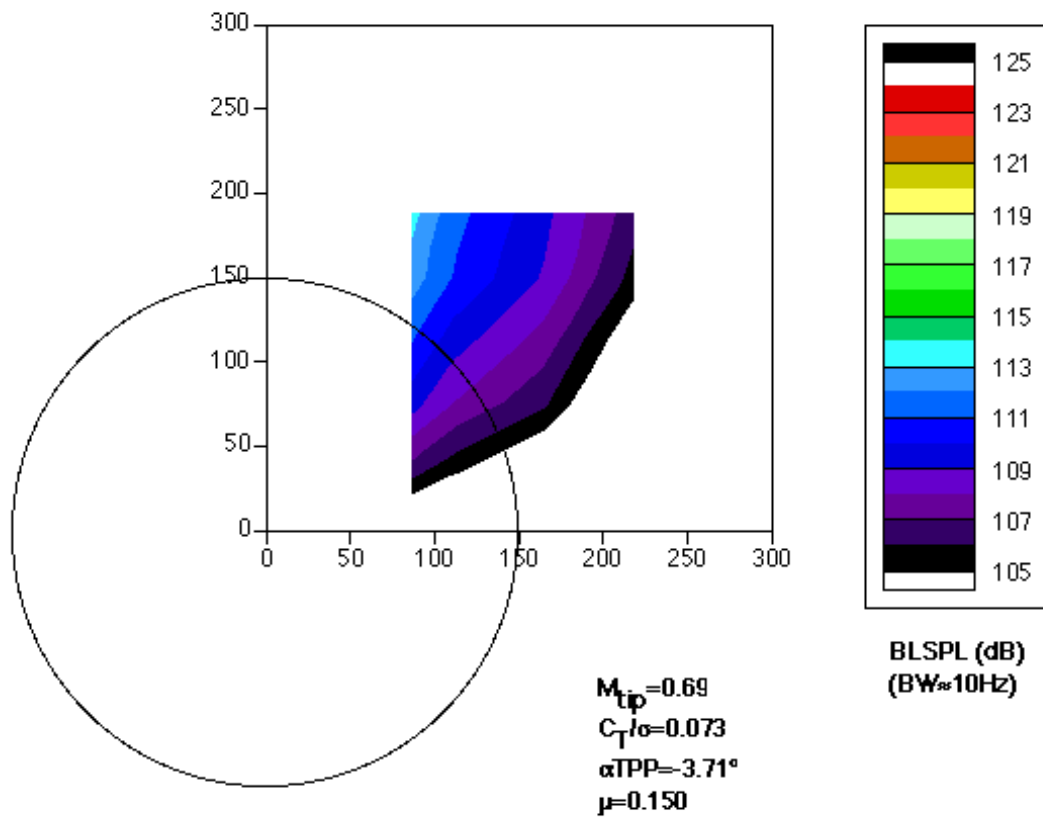


Fig 12. Continued.

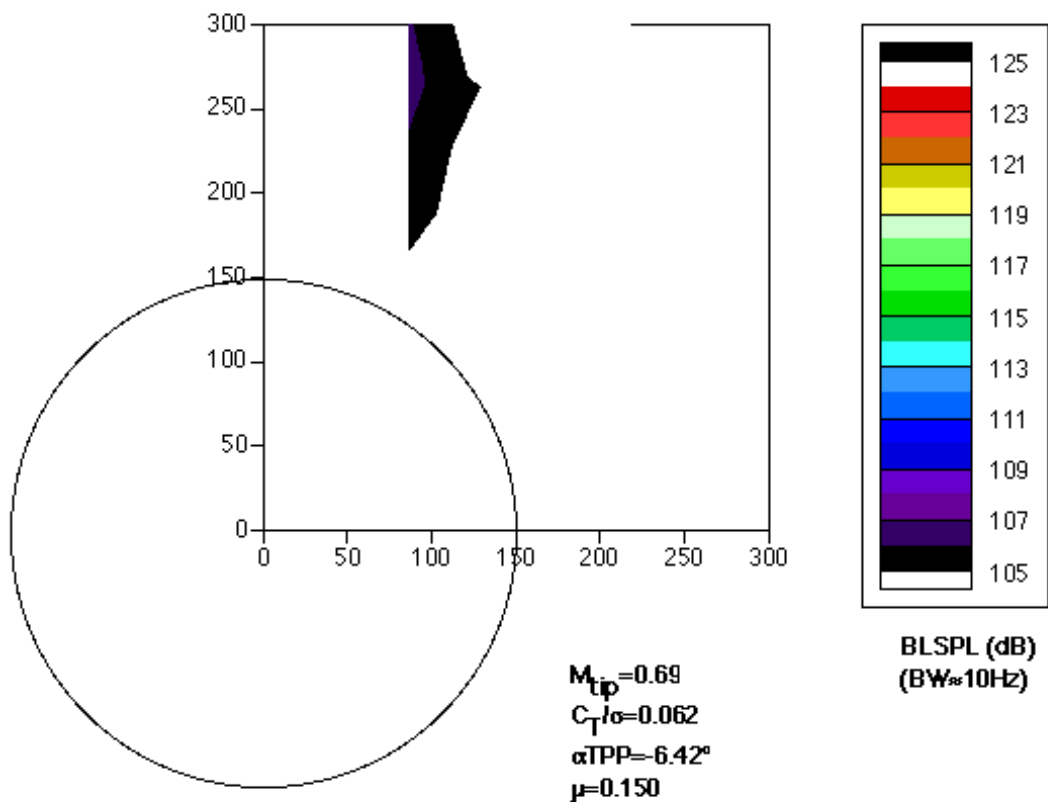


Fig 12. Concluded.

APPENDIX

XV-15 ACOUSTIC DATA FILES

All of the acoustic data from the full-scale XV-15 rotor test in the NASA Ames 80- by 120-Foot Wind Tunnel are provided on a CD-ROM. The CD has been produced in ISO 9660 format readable on a wide variety of computers. The files are in text format.

The file names reflect the specific Run and Point with reference to table 3. For example, file T832R12P020 refers to Test 832 (the XV-15 test), Run 12, Point 20.

The files are organized into four directories:

(1) The “-FA” directory contains the filtered (10th through 50th blade passage harmonics) averaged time histories. The microphone data values are Sound Pressure in Pascals. Each file contains a header row, followed by 2048 rows representing the 2048/rev sampling. The data are in tab delimited columns as follows:

Index	Rev	Azimuth	Mic#1.....	Mic#6
1				
2				
.				
.				
.				
2048				

Figure A.1 is a representative filtered, averaged time history.

(2) The “-PS” directory contains the unfiltered, time-averaged power spectra. Each file contains a header, followed by approximately 400 rows representing the 400 blade-passage harmonics (up to the 4 kHz anti-aliasing filter limit). The data are in tab delimited columns as follows:

Order	Frequency (Hz)	Mic#1.....	Mic#6
1			
2			
.			
.			
.			
400			

Note that the values in these spectra files are in units of sound power (sound pressure squared) in Pascals². To obtain the equivalent decibel values, the following conversion must be made:

$$dB = 10 * \log10(p^2/(2e-5)^2)$$

where p^2 is the value in the file (units of Pascal²). Figure A.2 is a representative unfiltered, averaged power spectrum, including the corresponding background noise spectrum.

(3) The “-dBA” directory contains, in seven files, one for each of the data runs, the A-weighted sound power metric (dBA) values for each data point and microphone. Each file contains a header row, followed by a variable number (depending on the number of data points obtained during that particular run) of rows of dBA data. The data are in tab delimited columns as follows:

Point	Mic#1	Mic#6
0n		
.		
.		
.		
nn		

(4) The “-F2_BLdB” directory contains, in six files, one for each of the data runs, the band-limited (filtered 10th through 50th blade-passage harmonics) sound power metric (BLSPL) values for each data point and microphone. Each file contains a header row, followed by a variable number (depending on the number of data points obtained during that particular run) of rows of BLSPL data. The data are in tab delimited columns as follows:

Point	Mic#1	Mic#6
0n		
.		
.		
.		
nn		

Note that only unfiltered power spectra of background noise (Run 19) data are included. Therefore, “T832R19Pnn-xx.dat” files appear only in the “-PS” and “-dBA” directories.

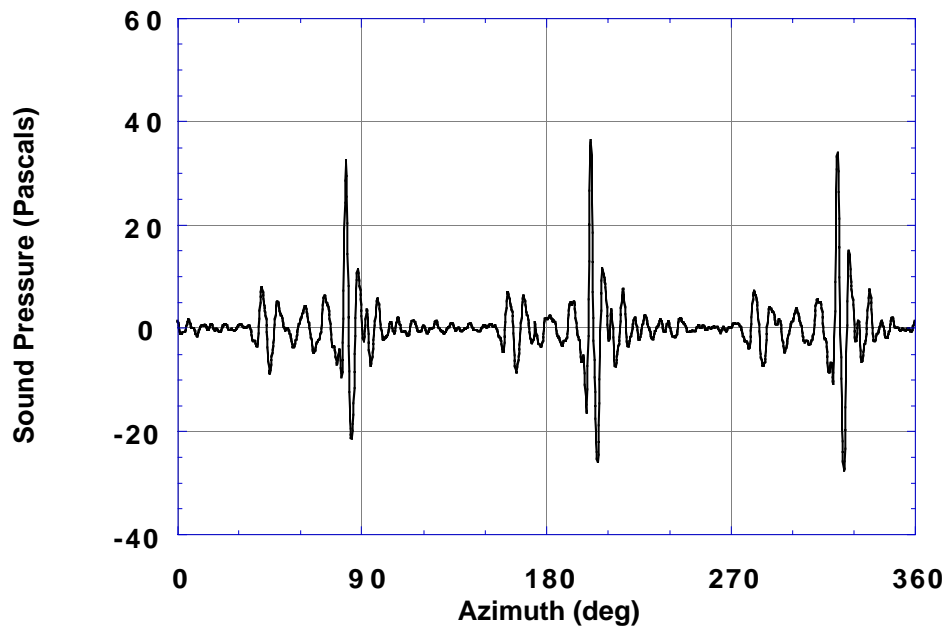


Fig A.1. Filtered, averaged time history. Run 12, Point 65 ($M_{tip} = 0.69$, $C_T/\sigma = 0.076$, $\mu = 0.177$, $\alpha_{TPP} = 3.04^\circ$), Mic #5.

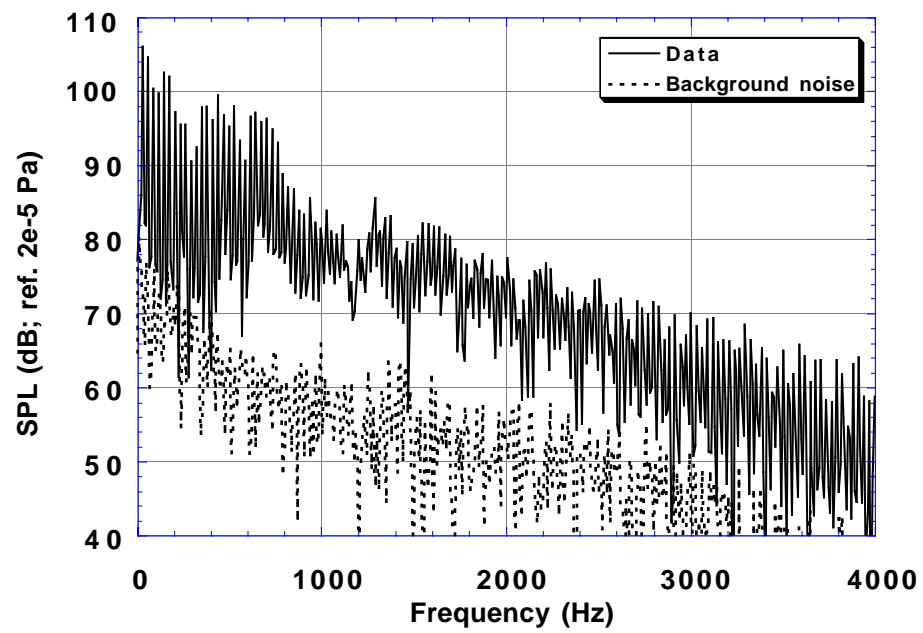


Fig A.2. Unfiltered sound power spectrum for Run 12, Point 65, Mic #5.

REPORT DOCUMENTATION PAGE

Form Approved
OMB No. 0704-0188

Public reporting burden for this collection of information is estimated to average 1 hour per response, including the time for reviewing instructions, searching existing data sources, gathering and maintaining the data needed, and completing and reviewing the collection of information. Send comments regarding this burden estimate or any other aspect of this collection of information, including suggestions for reducing this burden, to Washington Headquarters Services, Directorate for Information Operations and Reports, 1215 Jefferson Davis Highway, Suite 1204, Arlington, VA 22202-4302, and to the Office of Management and Budget, Paperwork Reduction Project (0704-0188), Washington, DC 20503.

1. AGENCY USE ONLY (Leave blank)	2. REPORT DATE	3. REPORT TYPE AND DATES COVERED	
	July 1999	Technical Memorandum	
4. TITLE AND SUBTITLE		5. FUNDING NUMBERS	
Blade-Vortex Interaction Noise of a Full-Scale XV-15 Rotor Tested in the NASA Ames 80- by 120-Foot Wind Tunnel		581-10-12	
6. AUTHOR(S)			
C. Kitaplioglu			
7. PERFORMING ORGANIZATION NAME(S) AND ADDRESS(ES)		8. PERFORMING ORGANIZATION REPORT NUMBER	
Ames Research Center Moffett Field, CA 94035-1000		A-99V0029	
9. SPONSORING/MONITORING AGENCY NAME(S) AND ADDRESS(ES)		10. SPONSORING/MONITORING AGENCY REPORT NUMBER	
National Aeronautics and Space Administration Washington, DC 20546-0001		NASA/TM-1999-208789	
11. SUPPLEMENTARY NOTES Point of Contact: C. Kitaplioglu, Ames Research Center, MS T12B, Moffett Field, CA 94035-1000 (650) 604-6679			
12a. DISTRIBUTION/AVAILABILITY STATEMENT Unclassified — Unlimited Subject Category 05 Availability: NASA CASI (301) 621-0390		12b. DISTRIBUTION CODE Distribution: Standard	
13. ABSTRACT (Maximum 200 words) A full-scale isolated XV-15 rotor was tested in the NASA Ames 80- by 120-Foot Wind Tunnel to determine the baseline blade-vortex interaction (BVI) noise signature at typical descending flight conditions. The test is briefly described. Representative samples of the acoustic data are presented. All of the acoustic data are included on an enclosed CD-ROM.			
14. SUBJECT TERMS Rotorcraft, Acoustics, Blade-vortex interaction, XV-15		15. NUMBER OF PAGES 51	
		16. PRICE CODE A04	
17. SECURITY CLASSIFICATION OF REPORT Unclassified	18. SECURITY CLASSIFICATION OF THIS PAGE Unclassified	19. SECURITY CLASSIFICATION OF ABSTRACT	20. LIMITATION OF ABSTRACT